The Proline-Rich Family Protein EXTENSIN33 Is Required for Etiolated Arabidopsis thaliana Hypocotyl Growth

Malgorzata Zdanio, Agnieszka Karolina Boron, Daria Balcerowicz, Sébastjen Schoenaers, Marios Nektarios Markakis, Grégory Mouille, Isabel Pintelon, Dmitry Suslov, Martine Gonneau, Herman Höfte, et al.

The proline-rich family protein EXTENSIN33 is required for etiolated Arabidopsis thaliana hypocotyl growth

Title: The Proline-rich Family Protein EXTENSIN33 Is Required For Etiolated *Arabidopsis thaliana* Hypocotyl Growth

Running head: EXTENSIN33 regulates Arabidopsis hypocotyl growth

Corresponding author: K. Vissenberg; Biology Department, Integrated Molecular Plant Physiology research, University of Antwerp, Groenenborgerlaan 171, Antwerpen, 2020, Belgium, phone: 003232653410, Email: kris.vissenberg@uantwerpen.be

Subject area: growth and development

Black and white figures: 0

Colour figures: 5

Tables: 2

Supplementary material: 6 supplemental figures

Title: The Proline-rich Family Protein EXTENSIN33 Is Required For Etiolated *Arabidopsis thaliana* Hypocotyl Growth

Running head: EXTENSIN33 regulates Arabidopsis hypocotyl growth

Malgorzata Zdanio[1], Agnieszka Karolina Boron[1,$], Daria Balcerowicz[1], Sébastjen Schoenaers[1], Marios Nektarios Markakis[1], Grégory Mouille[2], Isabel Pintelon[3], Dmitry Suslov[4], Martine Gonneau[2], Herman Höfte[2], Kris Vissenberg[1,5,*]

[1] Biology Department, Integrated Molecular Plant Physiology research, University of Antwerp, Groenenborgerlaan 171, 2020 Antwerpen, Belgium

[2] Institut Jean-Pierre Bourgin, INRA, AgroParisTech, CNRS, Université Paris-Saclay, 78000, Versailles, France

[3]Laboratory of Cell Biology and Histology, Department of Veterinary Sciences, University of Antwerp, Universiteitsplein 1, 2610 Wilrijk, Belgium

[4] Saint Petersburg State University, Faculty of Biology, Department of Plant Physiology and Biochemistry, Universitetskaya emb. 7/9, 199034 Saint Petersburg, Russia

[5] Plant Biochemistry & Biotechnology Lab, Department of Agriculture, Hellenic Mediterranean University, Stavromenos PC 71410, Heraklion, Crete, Greece

[*] Corresponding author: kris.vissenberg@uantwerpen.be

[$] Present address : Scion, Rotorua, New Zealand

ABSTRACT

Growth of etiolated Arabidopsis hypocotyls is biphasic. During the first phase, cells elongate slowly and synchronously. At 48hrs after imbibition, cells at the hypocotyl base accelerate their growth. Subsequently, this rapid elongation propagates through the hypocotyl from base to top. It is largely unclear what regulates the switch from slow to fast elongation. Reverse genetics-based screening for hypocotyl phenotypes identified three independent mutant lines of At1g70990, a short extensin family protein which we named EXT33, with shorter etiolated hypocotyls during the slow elongation phase. However, at 72hrs after imbibition, these dark-grown mutant hypocotyls start to elongate faster than the wild type. As a result, fully mature 8-day-old dark-grown hypocotyls were significantly longer than wild types. Mutant roots showed no growth phenotype. In line with these results, analysis of native promoter-driven transcriptional fusion lines revealed that in dark-grown hypocotyls expression occurred in the epidermis and cortex and that it was strongest in the growing part. Confocal and spinning disk microscopy on C-terminal protein-GFP fusion lines, localized the EXT33-protein to the ER and cell wall. Fourier Transformed Infrared (FT-IR) Microspectroscopy identified subtle changes in cell wall composition between wild type and the mutant, reflecting altered cell wall biomechanics measured by constant load extensometry. Our results indicate that the EXT33 short extensin family protein is required during the first phase of dark-grown hypocotyl elongation and that it regulates the moment and extent of the growth acceleration by modulating cell wall extensibility.

Key words: *Arabidopsis thaliana*, cell wall, etiolated hypocotyl growth, FT-IR analysis, short extensin, creep test

INTRODUCTION

Since higher plants are sessile, they have evolved an adaptive developmental program that allows them to grow in balance with the continuously changing environment. Ultimately, growth is the result of two processes, an increase in the number of cells by cell division and an increase in the volume by cell expansion (Lyndon 1990). Many studies on both processes exploit the model plant *Arabidopsis thaliana*. One of its organs, the hypocotyl, is widely used for research on the elongation process, since all its meristematic divisions are finished in the embryo before desiccation of the and since its growth in the dark is very prominent (Scheres et al. 1994; Boron et al. 2014). The cells in these dark-grown hypocotyls pass through two distinct growth phases. During the first phase, cells appear to be in a transition state and they all grow slowly. At 48hrs after seed imbibition, cells at the base of the hypocotyl undergo a growth acceleration and elongate rapidly (Refrégier et al. 2004). Subsequently, neighboring cells repeat this acceleration, resulting in a zone of growth acceleration that moves acropetally. The onset of fast elongation can be inhibited by cellulose synthase inhibitors, but only when applied before the growth acceleration, which suggests that prior to the acceleration, cells need to be prepared to be able to start fast elongation and secondly that expansion and cell wall synthesis are uncoupled during the second phase (Gendreau et al. 1997). To identify genes that are involved in the different phases of hypocotyl elongation, a micro-array analysis was performed before, during and after the switch from slow to fast elongation. This approach identified a list of differentially expressed genes, which indicates that just before the growth acceleration the expression of ribosomal genes decreases and that many auxin-regulated genes become up-regulated. Among the up-regulated genes many encode cell wall modifying proteins, which belong to the families of expansins, xyloglucan endotransglucosylase/hydrolases (XTHs), pectin-modifying enzymes and hydroxyproline-rich glycoproteins (HRGPs) (Pelletier et al. 2010).

The superfamily of HRGPs is subdivided into three groups, based on the pattern of proline hydroxylation and the level of glycosylation, namely arabinogalactan proteins (AGPs), proline-rich proteins (PRPs) and extensins (EXTs) (Ihsan et al. 2017). Their primary amino acid sequence, especially regarding the location and distribution of proline residues, poses a crucial criterion for their classification. In addition, the abundance of distinct and highly repetitive protein motifs enables researchers to employ bioinformatics approaches to analyse and identify particular HRGPs.

The major family of HRGPs consists of hyperglycosylated AGPs and is represented by 85 different proteins in the *Arabidopsis thaliana* proteome. AGPs typically exhibit sequences of non-contiguous proline residues (e.g. SPSPSP), and these motifs are hydroxylated and subsequently glycosylated by either short arabino-oligosaccharides or markedly longer arabinogalactan (AG) polysaccharides (Liu et al. 2016). The role of AGPs is mostly attributed to their adhesive properties (Tan et al. 2018; Lamport and Varnai 2013). In an ion-regulated mechanism, they maintain the integrity between the cell wall and plasma membrane during cell wall loosening processes, and due to the presence of a GPI anchor, AGPs are also involved in signal transduction as putative co-receptors (Zhang et al. 2011).

The PRP family is the least documented class of HRGPs and consists of 18 Hyp/Pro-rich proteins (H/PRPs) in *Arabidopsis thaliana* (Showalter et al. 2010; Hijazi et al. 2014). PRPs contain repetitive regions of adjacent proline residues. In contrast to AGPs, not all PRPs undergo post-translational modifications and can be classified as non- or weakly-glycosylated HRGPs. The latter carry side chains of only arabino-oligosaccharides. The classification of *Arabidopsis thaliana* PRP genes is based on their DNA sequence similarity, repetitive protein regions and domain organization (Fowler et al. 1999). Major functions attributed to PRPs are their involvement in the control of plant development and defense against biotic and abiotic stresses (Bradley et al. 1992; Bernhardt and Tierney 2000; Battaglia et al. 2007). The first description of PRPs mentions that they accumulate in carrot root cell walls after physical damage (Chen and Varner 1985; Tierney et al. 1988). In *Arabidopsis* four PRP genes are well characterized, and they encode two unique groups of PRPs. Both *AtPRP1* and *AtPRP3* are expressed in roots, and *AtPRP3* is specifically localized in root hair cells where the protein is involved in cell wall rearrangement and epidermal cell differentiation (Bergonci et al. 2014). Transcripts of *AtPRP2* and *AtPRP4* were detected in expanding leaves, stems, flowers, siliques, hypocotyls and cotyledons. Furthermore, AtPRP4 is associated with the establishment of a cell wall matrix during lateral root initiation. This class of structural cell wall proteins may be involved in interactions within the extracellular matrix and possibly with proteins within the cell membrane (Fowler et al. 1999). Their precise function remains, however, unknown. Based on sequence similarities with these four PRP genes, Boron et al. (2014) identified and characterized a proline-rich protein-like PRPL1 that, similar to *AtPRP3*, is involved in the control of root hair elongation. As for the other proteins, the working mechanism of *AtPRPL1* remains elusive.

The second and larger family of HRGPs is a group of 59 moderately glycosylated extensins (EXTs). EXTs, in contrast to AGPs, contain clusters of adjacent prolines (e.g., APPPP) that are hydroxylated and glycosylated only by short arabino-oligosaccharides. Forty five percent of the *Arabidopsis* EXT sequences contains cross-linking YXY motifs that can form isodityrosine *in vitro*, and this is clearly associated with plant development and defense mechanisms (Liu et al. 2016). The bioinformatics program BIO OHIO 2.0 subdivides EXTs into several clades based on amino acid composition: classical EXTs, leucine-rich repeat extensins (LRXs), proline-rich extensin-like receptor kinases (PERKs), formin-homolog EXTs (FH EXTs), long chimeric EXTs, other chimeric EXTs and short EXTs (Liu et al. 2016). Classical EXTs are characterized by a signal peptide that targets them to the secretory pathway and ultimately to the cell wall. However, most EXTs are of the non-classical type (LRXs, PERKs, FH EXTs, long chimeric EXTs, other chimeric EXTs), and they can be distinguished by the abundance of non-HRGP domains. Lastly, short EXT proteins contain less than 200 amino acids. Several of the 12 short EXT members in *Arabidopsis thaliana* contain a predicted C-terminal glycosylphosphatidylinositol (GPI) membrane anchor, attaching the protein to the outer plasma membrane leaflet. The precise function for the majority of EXTs remains unknown. Mutant analysis provided functional insight into the role of several other EXTs. A loss-of-function allele of AtEXT3 is seedling-lethal and yields a *root-, shoot-, hypocotyl-defective* (*rsh*) mutant (Hall et al. 2002; Cannon et al. 2008). In hypocotyls of *Brassica napus*, extensins were detected in cell walls that withstand tensile stress (Shirsat et al. 1996). Mutant analysis indicates that LRX1 and PERK13 function in root hair development and elongation of root cells, respectively (Baumberger et al. 2001; Humphrey et al. 2007).

In an attempt to better understand how the switch between the slow and the fast elongation of dark-grown hypocotyl is regulated, we used the micro-array data gathered by Pelletier et al. (2010) as a basis to perform a reverse genetics approach. We obtained and analysed mutants in the genes that are upregulated just before the start of fast hypocotyl elongation or downregulated once fast elongation has started, and we used the length of etiolated hypocotyls as the selection criterion. This approach has led to the identification of At1g70990, which we named EXT33, a short extensin family protein being involved in the regulation of hypocotyl growth through subtle changes in cell wall characteristics.

RESULTS

Identification and characterization of 3 mutant alleles of At1g70990, named *EXT33*.

To characterize potential regulators of hypocotyl growth, we used a reverse genetics approach based on genes that were identified by the micro-array analysis performed by Pelletier et al. (2010). Homozygous lines for each individual T-DNA insertion line were grown in the dark and the length of 8-day-old hypocotyls was measured and compared to the wild type. This phenotypic screening identified SALK-lines N663130-4, N666962-2 and N65726 with significantly longer hypocotyls than the wild type (Fig. 1A-C). PCRs coupled to DNA sequencing revealed that in N663130-4 and N666962-2 the T-DNA had been inserted in the promoter region of At1g70990, while in N65726 the T-DNA had been inserted in the only exon of the same gene (Fig. 1D).

The At1g70990 gene contains no introns and has an ORF of 528bp that encodes a protein of 176 amino acids (Fig. 1D). At1g70990 belongs to the class of 12 short EXTs (Showalter et al. 2010) and was therefore named *EXT33*. Borner et al. (2002) predicted that the EXT33-protein (AAD55511.1) putatively belongs to GPI-anchored proteins in Arabidopsis and it was included in the group of six identified extensin-related proteins, being all members of the AtPRPs subfamily. Glycosylphosphatidylinositol (GPI)-anchoring of proteins normally targets them to the plasma membrane where they extend their major domains into the cell wall, so that they are likely involved in extracellular matrix remodeling and signaling (Borner et al. 2002; 2003). Alignment of EXT33 and other well-known AtPRPs, however, does not point to significant similarities and rather suggests the absence of a GPI-anchor. In addition, bio-informatic analysis shows that EXT33 contains two pentapeptide repeats (SP4) and a single YXY repeat (Fig. 1E), which can be involved in EXT cross-linking. Using a BLASTP similarity search (Altschul et al. 1990, 1997) and the EXT33 sequence as a query sequence, phylogenetic analysis showed that within the short EXTs family, the best protein matches are At1g02405 (EXT30) and At1g23040 (EXT31) with protein similarities of 51.1% and 56.8%, respectively (Fig. 1E). The GPI-anchor predicting tool PredGPI (Pierleoni et al. 2008) indicates that similarly to EXT33, both EXT30 and EXT31 do not contains a GPI-anchor (data not shown). Phylogenetic trees containing best matches from only *Arabidopsis thaliana* proteins (Fig. 1F), all *Arabidopsis* taxa proteins (Fig. 1G) and only the subfamily of short EXTs (Fig. 1H) were constructed with the neighbor-joining method using MEGA5.05 (Tamura et al. 2011). Domain analysis using UniProt and INTERPRO predicts that EXT33 possesses two transmembrane helices (TMHx) in positions 48-66aa and 157-175aa. EXT33 has 36 proline residues (or 20%; see grey marked Ps in Fig. 1E) and a length of 176 amino acids, whereas EXT31 and EXT30 have 23% and 27% proline residues and a length of 144 and 134 amino acids, respectively. All three proteins share similarity within the predicted transmembrane helixes. However, the signal peptide that is present in both EXT30 and EXT31 seems absent in EXT33. Bio-informatic analysis using BIO OHIO 2.0 predicts that the N-terminal sequence of EXT33 does not act as a signal peptide. Other reports mention that the protein structures of EXTs contain several extremely conserved repetitive motifs, but that the N-terminal domain is indeed often variable.

Since At1g70990 encodes EXT33, we named SALK-lines N663130-4, N666962-2 and N65726 as *ext33-1*, *ext33-2* and *ext33-3*, respectively, and we will use these names in the remainder of the manuscript.

Altered *EXT33* expression increases etiolated hypocotyl cell expansion.

We confirmed that the T-DNA insertion caused a nearly complete knock-down of *EXT33* in the 3 lines (reduction by more than 81%, 75% and 85%, respectively (Fig. 2A). As 8-day-old dark-grown hypocotyls of *ext33-1*, *ext33-2* and *ext33-3* T-DNA lines were respectively 26%, 12% and 38% longer than the wild type, we analysed their growth in detail (Fig. 2B-D). Interestingly, during the first phases of growth, their hypocotyls remained shorter. This detailed time course experiment revealed that dark-grown hypocotyls of those mutants had higher growth rates during the third, fourth and fifth day after imbibition. This is the time when the mutant hypocotyls catch up, equal and at the end even surpass the length of the wild type. After the third-fourth day, growth rates of T-DNA insertion lines and WT became lower (Fig. 2E-G), resulting in practically complete cessation of hypocotyl growth by day eight (Fig. 2B-D). Comparison of the growth rate profiles shows that they are highly similar, but that only the absolute values of the growth rates are different between the WT and the mutants. This suggests that the boundary between the first and second growth phase is not shifted in time. When grown in the light, no statistically significant difference was found between mutant and wild type hypocotyls (data not shown). Similarly, no root growth phenotypes were detected in 3-, 6-, 8-, and 10-day-old seedlings (Fig. 2H-J), suggesting that EXT33 is especially required in the regulation of etiolated hypocotyl growth.

Since a lowered expression of *EXT33* had a striking effect on etiolated hypocotyls, we created *EXT33*-overexpression lines under control of the 35S-promoter and compared the growth of their hypocotyls with the wild type. We used 3 independent overexpression lines, 35S::EXT33-22, 35S::EXT33-13 and 35S::EXT33-24, where the *EXT33*-expression was 2.9, 1.8 and 2.8 times that of the wild type, respectively (Fig. 2A). Dark-grown hypocotyls were significantly longer than WT from 72 hrs onwards, while they behaved similarly to wild type during the earlier stages (Fig. 2K-M). In addition, light-grown hypocotyls of overexpression lines behaved exactly as the WT (data not shown). Changes in hypocotyl length can be caused by alterations in cell division activity (resulting in more cells), in cell expansion activity (resulting in longer cells) or both. To understand the cellular basis of this different etiolated hypocotyl growth in mutants and the wild type, we verified the number of cells in individual hypocotyl cell files. For

WT the average cell number was 22.43 ± 0.22, for *ext33-1* this was 22.31 ± 0.19, for *ext33-2* 21.50 ± 0.17 and for *ext33-3* 23.13 ± 0.21 (average ± SE). Thus, the altered growth in the mutants was not the result of extra rounds of cell division creating more cells per cell file, but solely of altered cell elongation.

The etiolated hypocotyl growth phenotype of *ext33*-mutants can be reversed by reintroducing EXT33.

Although the three different T-DNA insertion lines showed very similar etiolated hypocotyl growth, we nevertheless wanted to add additional proof that it is the lowered expression of *EXT33* that is causing the observed growth phenotypes. We therefore transformed the 35S::EXT33-GFP construct into the mutants, and performed a detailed growth analysis of etiolated hypocotyls of two independent homozygous lines. This showed no significant difference versus wild type in the first phase of elongation and confirms that the aberrant growth of the mutants in this phase is indeed caused by the lowered *EXT33*-levels. As for the 35S-lines created in the wild type background, the hypocotyls reached a longer length at the end of their growth (Suppl. Fig. 1A) and similarly, the expression levels of EXT33 in these lines (Suppl. Fig. 1B) approached the level of the 35S-lines represented in figure 2A.

***EXT33* is expressed in distinct cell types of hypocotyls, roots and in cotyledons.**

In silico analysis using eFP-browser predicts that *EXT33* is weakly expressed in the hypocotyl, while a stronger expression can be expected in the young embryo and cotyledons, and in the cortical and inner cell layers of the young root (Winter et al. 2007; Suppl. Fig. 2). *EXT33* then remains highly expressed in stele cells of older root parts. To confirm the spatiotemporal expression pattern, $\text{promoter}_{\text{EXT33}}$::GFP lines were created using a fragment of 1240bp upstream of the ATG start codon as the putative promoter-region. Several independent $\text{promoter}_{\text{EXT33}}$::GFP lines were grown in light and dark conditions and their GFP signal was visualized at different developmental stages. In 2-day-old seedlings *EXT33* expression was detected in the hypocotyls, cotyledons and in the root, irrespective of light conditions (Fig. 3A light, 3C dark). In case of light-grown seedlings the GFP signal was expressed throughout the hypocotyls, with especially strong expression in their basal part, while weak expression was seen in the cotyledons (Fig. 3A). In the young root, expression was observed in the stele and the cortex, which was confirmed on confocal cross-sections (Fig. 3D) that indicate expression of *EXT33* in the vascular tissue, endodermis and pericycle. In older root parts, expression was still detectable in the stele. Interestingly, the strongest expression signal was detected in the basal part of 2-day-old dark-grown hypocotyls (Fig. 3C), suggesting that this transcription of *EXT33* corresponds to the region of cells that start growth acceleration. When the GFP-fluorescence levels were quantified along the length in older dark-grown hypocotyls, the zone with the highest expression coincided with the fast-growing zone (Suppl. Fig. 3). This is in line with our observed growth defects in the earlier stages of etiolated hypocotyl growth in the *ext33* mutants (Fig. 2B-D). Cross-sections of dark-grown hypocotyls showed that GFP is localized in the epidermal and the first layers of cortical cells (Fig. 3E). Analysis of 5-day-old hypocotyls shows that *EXT33* expression levels decrease after the onset of fast elongation, but that expression remains detectable until hypocotyls are fully mature with their growth having ceased (Fig. 3B light).

GFP-tagged EXT33 localizes to the ER and cell wall.

Transgenic 35S-driven lines with a stable expression of N- or C-terminal GFP-tagged EXT33 were created and used to determine the subcellular localization of EXT33 using confocal microscopy. Only the C-terminal GFP-fusion lines showed a detectable GFP signal that was located in the ER of root (Fig. 4A) and dark-grown hypocotyl cells (Fig. 4B). We confirmed the localisation of the fusion-protein in roots (Fig. 4C) and hypocotyls (Fig. 4D) of 35S::EXT33-GFP reintroduced into *ext33*, and confirmed the location to be the ER using the ER-stain $DioC_6(3)$(Verbelen et al., 2001; Suppl. Fig. 4). However, as GFP is sensitive to pH and the cell wall is known to be an acidic compartment, we incubated the lines in a buffer at pH 8 and localized EXT33-GFP to the same location as propidium iodide in etiolated hypocotyl cells (Fig. 4E), a staining that is specific for pectin calcium-binding sites. In addition, incubation at pH was detrimental to the normal shape of the ER.

To ensure that GFP was bound to EXT33-protein, we performed Western Blot analysis on proteins extracted from C-terminal GFP-fusion lines with an anti-GFP antibody. Free GFP was detected at a size of 27 kDa. The expected size of the EXT33 protein is 19.4kDa, which, together with bound GFP, would result in an EXT33-GFP fusion-protein with a size of 46.4kDa. This corresponds to the upper band detected on the Western Blot. Our analysis therefore revealed that the majority of GFP is bound to EXT33, while only a small fraction of the observed GFP represents free GFP (Suppl. Fig 5). This is further confirmed by the observation that while cytoplasmic free GFP enters the nucleus, GFP was not detected inside the nucleus (suppl. Fig. 6).

FT-IR analysis identifies cell wall changes in At1g70990 alleles

Since changes in cell wall composition and arrangement of individual components can greatly impact on cell wall biomechanics and thus growth potential, a Fourier Transformed Infrared (FT-IR) Microspectroscopy analysis was performed on wild type and *ext33*-mutant cell walls. IR absorbance spectra were taken next to the central cylinder in the top, middle and basal part of 4-day-old etiolated hypocotyls and compared with the wild type using one-sample t-tests on the absorbance values at each single wavenumber (Fig. 5). This analysis suggests slight changes in cell wall composition between wild type and the mutants (Fig. 5A-C). Significant differences in IR-absorbances can be detected between wavenumbers 1700 and 1600 cm^{-1} and 1570 and 1480 cm^{-1}, corresponding to amide I (protein) (1650 and 1550 cm^{-1}) (Séné *et al.*, 1994), and phenolic rings (1630 and 1515 cm^{-1}) (Carpita et al. 2001), respectively. A significant decrease was seen at wavenumber 1758 cm^{-1}. The exact cell wall compound that corresponds to this peak is not described, but the closest known peak is at wavenumber 1740 cm^{-1}, which represents esterified uronic acids (McCann et al. 1992). In the middle part of hypocotyls from the line N666962-2 a significant decrease can be seen at 1369 and 1319 cm^{-1}, corresponding to changes in cellulose (1320 and 1367 cm^{-1}) (Kacuráková et al. 2000; Wilson et al. 2000; Carpita et al. 2001). Taken together, these data indicate that different T-DNA lines of *EXT33* may contain more proteins and phenolic compounds in their hypocotyl cell walls, and less esterified uronic acids and cellulose.

Constant load extensometry indicates that *ext33* mutants have more extensible walls

To reveal whether the observed changes in cell wall composition alter cell wall mechanics in the *ext33*-mutant hypocotyls, which in turn could explain the growth phenotypes, 5-mm long etiolated hypocotyl segments of 96h-old hypocotyls were extended in an extensometer (Suslov and Verbelen 2006), under a 600mg load. This load is optimal for hypocotyls of etiolated Arabidopsis seedlings, because it produces easily detectable *in vitro* wall extension with acceptably low frequency of sample failures (Boron et al. 2015). Measurement of cross-sectional areas of both mutant and wild type hypocotyls revealed no differences, indicating that the 600mg load creates the same stress in mutant and wild type walls and therefore enables direct comparison of their responses to the applied load. Creep rates, expressed as percentage of extension per hour (Fig. 5D), of both mutant segments were significantly higher than those of the wild type, suggesting that the mutant walls were more extensible than wild type cell walls.

DISCUSSION

Plant cells synthesize many non-enzymatic proteins that are implicated in the structure and mechanical properties of the cell wall. One of the most abundant groups of structural proteins is a superfamily of HRGPs. Their features, especially the presence of an YXY motif, enables the formation of cross-links in the cell wall (Hijazi et al. 2014). However, despite comprehensive study, the function of many HRGPs remains poorly understood.

This work aims to characterize At1g70990, which encodes a protein that is required for the initial slow elongation phase of hypocotyl cells based on time course gene expression data from Pelletier et al. (2010) and from our mutant phenotyping experiments. Literature stated that At1g70990 belongs to GPI-anchored proteins of the HRGP superfamily in *Arabidopsis*, and it was initially classified as a proline-rich protein (PRP) (Borner et al. 2002). However, amino acid sequence alignment with known proline-rich proteins does not show any similarities. In addition, phylogenetic analysis showed that At1g70990 is most closely related to At1g02405 (EXT30) and At1g23040 (EXT31), both genes that belong to the class of short extensins. Those findings confirm previous results (see Supplemental data of Showalter et al. 2010), where a bio-informatic tool was developed in order to declutter biological data and to establish a classification of HRGPs. We therefore conclude that At1g70990 is a short extensin and that it can be named EXT33.

The function as well as the expression pattern of one of its closest relatives, EXT30, have not been determined yet. Moreover, little is known about EXT31, except that it appears to be highly up-regulated in mature Arabidopsis trichomes and falls into a cluster of cell wall-related transcripts (Jakoby et al. 2008). EXT31 is also included in the list of defense-related genes highly activated after pathogen infection (Zhang et al. 2007). *In silico* analysis indicated that the EXT33 protein sequence does not contain an N-terminal signal peptide, but two potential internal transmembrane helices (TMHs). Furthermore, BLAST analysis shows that the N-terminal sequence of EXT33 does not match with sequences of its closest relatives EXT31 and EXT30, suggesting that the EXT33 protein cannot be targeted to a specific (sub)cellular location and that the present N-terminal sequence could assist in efficient expression and proper folding of the glycoprotein (Vembar and Brodsky 2008; Caramelo and Parodi 2015). Nevertheless, in protein-fusion lines we detected EXT33-GFP at the ER and in the cell wall, suggesting that EXT33's N-terminal part is active. We furthermore ensured that the observed GFP is bound to EXT33 using Western Blot analysis.

Analysis of promoter$_{EXT33}$::GFP lines suggests that *EXT33* expression is positively correlated with the growth phases of hypocotyl cells, which makes sense since the gene was identified based on a screen for hypocotyl growth-related genes (Pelletier et al. 2010). Several other papers mention that extensins are expressed in elongating hypocotyls. They accumulate in young soybean hypocotyls and are confined to cortex and cambium cells (Keller 1993; Ye and Varner 1991). In addition, Showalter et al. (1986) described the accumulation of HRGP mRNAs in biologically stressed melon and soybean hypocotyls. Other studies indicate that extensins are key regulators of plant defense responses against pathogen infections (Zhang et al. 2007).

Our mutant growth analysis shows that EXT33 is involved in fine-tuning elongation rates during the first phase of etiolated hypocotyl growth. Lowered expression of *EXT33* indeed led to initially shorter hypocotyls when compared to the wild type. This was followed by a rapid increase of the growth rate during the third, fourth and fifth day, which ultimately led to longer hypocotyls than those of the wild type after 96h. In addition, artificially increasing EXT33 levels in overexpression and protein-fusion lines (*EXT33(-GFP)* expression driven by the 35S promotor in WT or *ext33* background), showed that the second growth phase of hypocotyls was affected too, resulting in longer hypocotyls. These data indicate that EXT33 regulates both phases of cell elongation in etiolated hypocotyl cells in a complex manner.

Plant cell growth largely depends on cell wall composition and extensibility, both of which are potentially impacted on in *ext33*. FT-IR analysis indicates that EXT33 potentially modifies the cell wall indirectly since it resides in the ER and directly since it is found in the cell wall too. Subtle changes were detected in T-DNA mutant cell wall composition and *in vitro* wall extension. Mutant cell walls contained more proteins and phenolic compounds and less esterified uronic acids and cellulose. Among these changes the decrease in uronic acid esterification has the most obvious link with the growth stimulation in the mutant lines. Uronic acids are the main constituents of pectins, the load-bearing role of which has recently been re-established (Dick-Perez et al. 2011; Phyo et al. 2017). Pectin deesterification is considered to render this polymer more sensitive to polygalacturonase-mediated hydrolysis (Peaucelle et al. 2008). At the same time, polygalacturonases were shown to stimulate growth in Arabidopsis hypocotyls (Xiao et al. 2014, 2017). Whether this indirect mechanism actually explains the effect of absence and overexpression of EXT33 on growth is still to be determined. Given the ER-cell wall localisation of EXT33, it is speculative to mention that EXT33 is somehow involved in (the regulation of) the delivery of new cell wall material and/or modifying enzymes to the cell wall, acting as a kind of chaperone, or that it serves as a modulator of cell wall build up/modifications. As such, EXT33 may play a role in the construction of the thick wall during the slow growth phase. Without EXT33, the assembly is inefficient which slows down the growth or delays the transition, but once rapid growth is initiated the EXT33-less wall can be more easily extended. In this view, overexpression of EXT33 may actually accelerate wall assembly, in which case a thicker wall may have more growth capacity during the rapid growth phase. So, whereas in both cases (absence and overexpression of EXT33) the hypocotyl is longer, it can be through different mechanisms. However, as with other HRGPs, the exact mode of action remains elusive.

In summary, our work indicates that At1g70990 encodes the ER/apoplastic EXT33, a short extensin that regulates etiolated hypocotyl cell growth through subtle changes in cell wall composition and its biomechanics.

MATERIALS AND METHODS

Plant material and growth conditions

Arabidopsis thaliana seeds of the T-DNA insertion lines (Table 1) and Columbia 0 (Col-0; N1093) wild type were obtained from the Nottingham Arabidopsis Stock Centre (NASC) (Scholl et al. 2000). The seeds were sown on Tref Substrate soil upon arrival to bulk them up for further experiments. Seeds of homozygous lines were surface-sterilized in 6% commercial bleach solution for 5 min, washed with 96% EtOH and finally rinsed with 100% EtOH. Seeds were then left to dry in a laminar flow cabinet (GELAIRE, HF48).

To study dark-grown hypocotyls, dried seeds were placed on agar-solidified medium without sucrose according to Estelle and Somerville (1987), which consisted of 5 mM KNO_3; 2.5 mM KH_2PO_4; 2 mM $MgSO_4(7H_2O)$; 2 mM $Ca(NO_3)_2$; 70 mM H_3BO_3; 14 mM $MnCl_2$; 0.5 mM $CuSO_4(5H_2O)$; 0.2 mM $Na_2MoO_4(2H_2O)$; 10 mM NaCl; 1 mM $ZnSO_4(7H_2O)$; 0.01 mM $CoCl_2(6H_2O)$; 100 µg ml^{-1}myoinositol; 1 µg ml^{-1} calcium panthotenate; 1 µg ml^{-1}niacine; 1 µg ml^{-1} pyridoxine; 1 µg ml^{-1} thiamine HCl; 0.01 µg ml^{-1}biotine; 5 µg ml^{-1} ferric citrate (added after autoclaving); 0.07% MES, pH 6.0; 8 µg ml^{-1}bromocresol purple; and 0.7% agar. Subsequently, plates were closed with Parafilm (Parafilm, Pechiney Plastic Packaging, Menasha, WI, USA). After 3 days of stratification at 4°C, synchronous germination was induced by exposure to fluorescent white light (150 µmol m^{-2} s^{-1} True Light; Philips, Eindhoven, The Netherlands) during 6 hours at 21°C. The transfer to light is referred to as “induction” and is considered as t=0 for all the experiments. After the exposure to light, darkness was obtained by wrapping the Petri dishes in four layers of aluminium foil. Covered plates were placed vertically at 21°C in an environmentally controlled growth cabinet (cooled incubator BRC120, Bioconcept-Firlabo, Beun De Ronde, Drogenbos, Belgium).

To grow seedlings in the light, sterilized seeds were placed on half-strength Murashige and Skoog (½ MS) (Murashige and Skoog 1962) agar-solidified medium including vitamins (Duchefa, The Netherlands), supplemented with 10 gl^{-1} sucrose, pH adjusted to 5.7 with KOH and solidified with 7 gl^{-1}agar (Duchefa, The Netherlands). Subsequently, plates were closed with Parafilm (Parafilm, Pechiney Plastic Packaging, Menasha, WI, USA). After 3 days of stratification at 4°C, the Petri dishes were placed vertically in a growth chamber with a 16 h light/8 h dark cycle at a light intensity of 24 µmolm^{-2}s^{-1} (PAR, Philips tlm 65W/33) and a temperature of 24°C with a constant humidity of 70%.

DNA isolation

Genomic DNA was extracted from soil-grown T-DNA insertion lines and WT Col-0 plants according to the previously described modified protocol of Edwards et al. (1991). In brief, 1 or 2 leaves of two-week-old plants were collected in a 1.5 ml Eppendorf tube. Leaves from eight independent plants per T-DNA line were collected and they were homogenised in 400 µl of Edward's extraction buffer (200mM TRIS, pH 7.5; 250 mM NaCl; 20 mM EDTA;0.5% (w/v) SDS) using custom-made sterilized glass grinders. The samples were centrifuged at 13000 rpm for 2 min and 300 µl of supernatant was transferred to a new 1.5 ml Eppendorf tube before 300 µl ice–cold isopropanol (-80°C) was added. The samples were mixed by inverting and after 2 min at room temperature they were centrifuged at 13000 rpm for 5 min. The supernatant was then removed, and the pellets were dried in an oven at 37°C overnight. The genomic DNA was dissolved in 50 µl Milli-Q water and quantified using an Eppendorf BioPhotometer.

Genotype analysis

Seeds obtained from NASC were sown on soil and leaves from eight independent plants per T-DNA line were collected. Their genomic DNA was extracted according to the modified protocol of Edwards et al. (1991) and used in PCR reactions. PCRs were made with two pairs of primers. The first pair consisted of the left and right border primers specific for the gene and they anneal in the region flanking the T-DNA (Table 1). The second pair was made up by the right border primer specific for the gene and a T-DNA-specific primer LBb1.3 (5' ATTTTGCCGATTTCGGAAC 3'). These primer sets were used to discriminate between homozygous, heterozygous and wild type plants. The PCR products that resulted from the use of the right border gene specific primer and LBb1.3 were sent for sequencing at the VIB (Flemish Institute of Biotechnology). The sequencing results were blasted towards the Arabidopsis genome to identify the exact insertion position of the T-DNA.

Transcript analysis

qPCR analysis was performed to quantify the expression level of At1g70990 in the T-DNA insertion lines. RNA was isolated using TRIzol Reagent (Life Technologies) according to the guidelines of the manufacturer and the quality was checked with a nanodrop (ND1000). SuperScript TM II Reverse Transcriptase (Life Technologies) was used to perform cDNA synthesis according to the manufacturer's instructions. All samples were diluted 1:10 with RNAse-free water prior to the qPCR reaction. Gene expression analysis was performed using TaqMan Universal Master Mix II, with Uracil-N glycosylase (UNG) and ROX (passive reference dye) as a technical control. Specific TaqMan probes (Table 2) were used to quantify the expression of At1g70990. To normalise the samples the expression level of actin 8 (At1g49240) was monitored with the probe At02270958_gH. All probes were ordered from Life Technologies.

Results were analysed with the Step One Plus Real-Time PCR System (Life Technologies) software at a confidence level of 95%. At least two biological replicates and three technical replicates were measured.

Phenotype analysis

To study the effect of the T-DNA insertion on hypocotyl and root growth, homozygous T-DNA insertion lines of At1g70990 and wild type Col-0 seeds were grown on ES (Estelle and Somerville 1987) medium and treated as mentioned above. Photos of etiolated hypocotyls and roots were taken during 8 days at 1-day interval under safe green light to avoid any white light inhibition, using a digital camera (Canon, 50D). Manipulation of seedlings had no effect on hypocotyl/root growth or final length. Hypocotyl length was measured as the distance between the top of the root hairs around the collet and the base of the 'V' made by the petioles of the cotyledons (Scheres et al. 1994) using ImageJ (Abramoff et al. 2004). The root was measured from the junction with the hypocotyl. The data were statistically analysed using Student's two-tailed *t*-tests.

Determination of cell numbers in individual hypocotyl cell files

In order to verify the number of cells in separate hypocotyl cell files, plants of T-DNA insertion lines of At1g70990 and wild type Col-0 were grown under light conditions as described above. Pictures of 8-day-old seedlings were taken using differential contrast (DIC) microscopy, with a LEICA DM LB microscope (20x/0.5 HC PL Fluotar and 40x/0.75 HCS PL Fluotar). Images were analysed using the public domain image analysis software ImageJ (http://rsb.info.nih.gov/ij/). Two hypocotyl cell files were counted per seedling, starting from the cell above the root collet to the cell reaching the 'V' established by the cotyledon bases.

Generation of DNA constructs

To examine the tissue-specific and developmental expression pattern of At1g70990, promoter::GUS and promoter::GFP fusion constructs were created. All oligonucleotides were obtained from Eurogentech (Seraing, Belgium) and all constructs were made using Gateway® technology (Invitrogen™). The 1240bp sequence upstream of the ATG start codon was amplified by PCR with Platinum® Taq DNA Polymerase High Fidelity according to the manufacturer's instruction (Invitrogen™, Life Technologies) from BAC clone F15H11 (3600708/ AC008148) (Arabidopsis Biological Resource Center, ABRC). Primers used for amplifying the promoter region were forward primer LPat1g70990 (5' GGGGACAAGTTTGTACAAAAAAGCAGGCTCATATTTGGATTTGCATCTCTAGG 3') and reverse primer RPat1g70990 (5' GGGGACCACTTTGTACAAGAAAGCTGGGTGGGACTGATATACTAGCTAGTAC 3') including Gateway® technology compatible recombination sites (AttBs). The length of the amplified fragment was first checked on agarose gel before it was cloned into Gateway® pDONR™221 Vector (Invitrogen™). Obtained entry clones were transformed into One Shot® TOP10 Chemically Competent *Escherichia coli* cells (Invitrogen™). Clones with the correct insert were identified by colony PCR using a pair of vector-specific primers (M13 forward primer (5' GTAAAACGACGGCCAG 3'), and M13 reverse primer (5' CAGGAAACAGCTATGAC 3')). Correct entry-clones were used to clone the amplified region into the destination vectors pGWB3 (for promoter::GUS) and pGWB4 (for promoter::GFP) (Nakagawa et al. 2007). The constructs were sequenced to exclude PCR-errors. Final constructs were electroporated into *Agrobacterium tumefaciens* strain LBA 4404 (ElectroMAX™ *A. tumefaciens* LBA4404 Cells, Invitrogen™) harboring helper plasmid pAL4404 (Hoekema et al. 1983). *Arabidopsis thaliana* wild type (Col-0; N1093) plants were transformed by the flower dip method as described by Clough and Bent (1998), using a transformation buffer containing 5% sucrose, $MgCl_2 \cdot 6H_2O$(0.74gl^{-1}) and 0.02% (v/v) Silwet L-77 (polyalkyleneoxide modified heptomethyltrisiloxane) (GE Specialty Materials, Geneva, Suisse).

To determine the subcellular localization of the At1g70990-protein transgenic Arabidopsis plants bearing a protein-GFP fusion under control of a 35S promoter were constructed. The coding sequence of At1g70990 was ordered from GeneArt (Life Technologies) without the stop codon and recombined with destination vector pGWB5 (for 35S::At1g70990-GFP) and pGWB6 (for 35S::GFP-At1g70990) using Gateway-technology (Invitrogen)(Nakagawa et al. 2007). The final constructs were transformed into *Agrobacterium tumefaciens* and subsequently into *Arabidopsis thaliana* as described above.

After transformation, transgenic plants were selected on ½ MS medium (Murashige and Skoog 1962) supplemented with 1% sucrose, 0.7% agar (Duchefa, The Netherlands) and 50mgl^{-1} Kanamycin. For each construct, at least 28 independent transgenic lines were selected. Homozygous transgenic progeny was obtained after self-fertilizing and at least 5 different homozygous lines of the T_3 generation were identified and used in further experiments.

Confocal, spinning disk and macroscope microscopy

Seedlings were grown as mentioned before and they were imaged using a Nikon C1 confocal microscope (Nikon Eclipse E600 coupled to a D-Eclipse CA confocal unit; Nikon, Brussels, Belgium) using a 60x water immersion objective. Propidium iodide (0.1 mg l^{-1}) was used to stain the cell walls.

Images of 35S-driven C-terminal GFP fusions were also obtained using a Zeiss Axiovert 200 (Carl Zeiss, Jena, Germany) equipped with a microlens-enhanced dual spinning disk confocal system, using a three-line argon-krypton laser and a 63x oil immersion lens for higher resolution images (Ultraview ERS; Perkin Elmer, Seer Green, UK).

ER was stained using $DioC_6(3)$ as described in Verbelen et al. (2001).

PromEXT33::GFP lines were grown as mentioned before and they were imaged on a Nikon AZ100 macroscope equipped with a Nikon DS-Ri1 digital camera and using the 0.5x objective and a 100s exposure.

Phylogenetic analysis

To elucidate the relation of At1g70990 with other proteins a phylogenetic tree was created from parsimony analysis. The protein sequence of At1g70990 was used to retrieve related sequences from the BLAST program (Altschul et al.

1990). These retrieved sequences were aligned in ClustalW 1.87 and a phylogenetic tree was made from neighbor-joining analysis using Mega 5.05 software (Tamura et al. 2011). The bootstrap values are shown in the tree and 1000 replicates were used.

FT-IR analysis of dark-grown hypocotyls

FT-IR analysis was performed as described by Mouille et al. (2003) with the omission of the first step. Four-day-old dark-grown hypocotyls of wild type and T-DNA insertion lines of At1g70990 were collected in absolute ethanol, rehydrated for few hours in distilled water and air-dried at 37°C for at least 20 minutes. Four biological repeats were obtained and 5 spectra for each repeat were used to analyze cell wall composition. Spectra were taken at the base, middle and top part of the hypocotyls. The spectra were base line-corrected and area-normalized before further analysis as described in Mouille et al. (2003) but using R software. MeV 4.9 software was used to perform principal component analysis (PCA). One-sample-t tests (using R software) were executed to detect significant changes in the absorption at the different wavenumbers, which is indicative for compositional or structural changes in the cell walls.

Protein extraction and Western blot analysis

For protein extraction, 50 mg of 4 days dark-grown seedlings were ground into 100 µl of 4 M urea, 100 mM DTT extraction buffer and 50 µl of Laemmli loading buffer were added. The samples were boiled for 5 min and centrifuged at 10 000 g for 15 min at 4°C. Aliquots of the supernatant were loaded on NuPAGE™ 4-12% Bis-Tris protein gels (Invitrogen™) and proteins were separated using MOPS SDS running buffer (Invitrogen™) and then finally electro-transferred on PVDF membrane with the Trans-Blot® semi-dry transfer system (BioRad) according to standard protocols. For immunodetection, we used an anti-GFP antibody [3H9] (ChromoTek) and a goat anti-Rat IgG-HRP (Southern Biotech) at 1/5 000 dilution and 1/10 000 dilution respectively, and for tubulin as loading control, an anti-▯-tubulin (T5168, Sigma) and a goat anti-mouse HRP conjugated antibody (AC15-0360, AbCore) at 1/5 000 dilution and 1/10 000 dilution respectively. The signals were measured by chemiluminescence using the ECL Select™ Western blotting detection reagent and the LAS 4000 biomolecular imager from Fujifilm Life Science.

Constant load extensometry

To compare the biomechanics of wild-type and mutant hypocotyls, the constant-load (creep) method was used as described in Suslov et al. (2015). A 5 mm long hypocotyl segment (starting from 1.5 mm below the cotyledons) of 96 h old dark-grown hypocotyls was secured in the extensometer and preincubated in a 20 mM MES-KOH, pH 6.0 buffer in the relaxed state for two minutes, after which it was extended in the same buffer under a constant load (600 mg for 15 min). The relative creep rate (for brevity referred to as 'creep rate' below) was calculated with the formula provided in Miedes et al. (2013).

Five mm long segments (corresponding to those used in the creep test) were excised from fresh Arabidopsis hypocotyls with a custom-made double-bladed cutter for cell wall cross-sectional area determination. Between 60 and 80 hypocotyl segments were transferred to a container for critical point drying (Microporous Specimen Capsules and Caps; 120-200 µm pores, Electron Microscopy Sciences (EMS); AURION, Wageningen, The Netherlands). This cylindrical container with a lid is made from highly porous inert material easily permeable for organic solvents. Each container with hypocotyl segments was transferred to a separate borosilicate glass Petri plate, where the segments were extracted and dehydrated by four sequential 1 h washes in chloroform:methanol (1:1, v/v) followed by a 1 h wash in diethyl ether with subsequent air drying in a fume hood. The weight of the dry wall material prepared from 60-80 5 mm long segments of Arabidopsis hypocotyls was determined using a balance (SARTORIUS 2405, Germany) with a resolution of 1 µg. Cell wall cross-sectional areas were calculated from the weight of dry wall material as detailed in Suslov et al. (2015). The wild-type and the mutants used in the present study were found to have similar cross-sectional areas of their hypocotyl cell walls. Thus, the wall stress (the force acting on the wall divided by its cross-sectional area) induced during their uniaxial extension under a 600 mg load was also similar.

Statistical Analyses

All values reported in this work are the average of at least three independent biological replicates having at least 20 seedlings. Error bars represent standard errors. Statistical differences between control and each line were analysed using Student's t tests with paired two-tailed distribution and the P-value was taken at $P<0.05$, except where stated otherwise.

FUNDING

This work was supported by the Research Foundation–Flanders [FWO; G.002911N, G.0.602.11.N.10, 1.5.091.11.N.00 and G039815N to M.Z., K.V., and a post-doc fellowship to S.S.]; the University of Antwerp [BOF-IWS to A.K.B. and D.B.]; the Interuniversity Attraction Poles Programme – Belgian State – Belgian Science Policy [IUAP VI/33 to M.N.M. and K.V.]; and the Saint Petersburg State University [1.42.726.2017 to D.S.], and RFBR [19-04-00424 to D.S.].

DISCLOSURES

Conflicts of interest: No conflicts of interest declared

REFERENCES

Abramoff, M.D., Magelhães, P.J. and Ram, S.J. (2004) Image processing with ImageJ. *Biophot Internat.* 11: 36-42.

Altschul, S.F., Gish, W., Miller, W., Myers, E.W. and Lipman, D.J. (1990) Basic local alignment search tool. *J Mol Biol.* 215: 403–410.

Altschul, S.F., Madden, T.L., Schäffer, A.A., Zhang, J., Zhang, Z., Miller, W. and Lipman, D.J. (1997) Gapped BLAST and PSI-BLAST: a new generation of protein database search programs. *Nucl Acids Res.* 25: 3389-3402.

Battaglia, M., Solorzano, R.M., Hernandez, M., Cuellar-Ortiz, S., Garcia-Gomez, B., Marquez, J., et al. (2007) Proline-rich cell wall proteins accumulate in growing regions and phloem tissue in response to water deficit in common bean seedlings. *Planta* 225: 1121–1133.

Baumberger, N., Ringli, C. and Keller, B. (2001) The chimeric leucine-rich repeat/extensin cell wall protein LRX1 is required for root hair morphogenesis in Arabidopsis thaliana. *Gene Dev* 15: 1128-1139.

Bergonci, T., Ribeiro, B., Ceciliato, P.H.O., Guerrero-Abad, J..C, Silva-Filho, M.C. and Moura, D.S. (2014) Arabidopsis thaliana RALF1 opposes brassinosteroid effects on root cell elongation and lateral root formation. *J Exp Bot.* 65: 2219-2230.

Bernhardt, C. and Tierney, M.L. (2000) Expression of AtPRP3, a proline-rich structural cell wall protein from Arabidopsis, is regulated by cell-type-specific developmental pathways involved in root hair formation. *Plant Physiol.* 122: 705–714.

Borner, G.H., Sherrier, D.J., Stevens, T.J., Arkin, I.T. and Dupree, P. (2002) Prediction of glycosylphosphatidylinositol-anchored proteins in Arabidopsis. A genomic analysis. *Plant Physiol.* 129: 482-499.

Borner, G.H., Lilley, K.S., Stevens, T.J. and Dupree, P. (2003) Identification of glycosylphosphatidylinositol-anchored proteins in Arabidopsis. A proteomic and genomic analysis. *Plant Physiol.* 132 :568-577.

Boron, A.K., Van Loock, B., Suslov, D., Markakis, M.N., Verbelen, J.P. and Vissenberg, K. (2015) Over-expression of *AtEXLA2* alters etiolated Arabidopsis hypocotyl growth. *Ann Bot.* 115: 67-80.

Boron, A.K. and Vissenberg, K. (2014) The *Arabidopsis thaliana* hypocotyl, a model to identify and study control mechanisms of cellular expansion. *Plant Cell Rep.* 33: 697-706.

Bradley, D. J., Kjellbom, P. and Lamb, C.J. (1992). Elicitor-induced and wound induced oxidative cross-linking of a proline rich plant cell wall protein: a novel, rapid defense response. *Cell* 70: 21–30.

Cannon, M.C., Terneus, K., Hall, Q., Tan, L., Wang, Y., Wegenhart, B.L., Chen, L., Lamport, D.T.A. and Chen, Y. (2008) Self-assembly of the plant cell wall requires an extensin scaffold. *PNAS USA.* 105: 2226-2231.

Caramelo, J.J. and Parodi, A.J. (2015) A sweet code for glycoprotein folding. *FEBS Lett*. 589: 1873-3468.

Carpita, N.C., Defernez, M., Findlay, K., Wells, B., Shoue, D.A. and Catchpole, G. (2001) Cell wall architecture of the elongating maize coleoptile. *Plant Physiol.* 127: 551-565.

Chen, J. and Varner, J.E. (1985) Isolation and characterization of cDNA clones for carrot extensin and a proline-rich 33-kDa protein. *PNAS USA.* 82: 4399-4403.

Clough, S.J. and Bent, A.F. (1998) Floral dip: a simplified method for Agrobacterium-mediated transformation of *Arabidopsis thaliana*. *Plant J.* 16: 735-743.

Dick-Pérez, M., Zhang, Y., Hayes, J., Salazar, A., Zabotina, O.A. and Hong, M. (2011) Structure and interactions of plant cell-wall polysaccharides by two- and three-dimensional magic-angle-spinning solid-state NMR. *Biochem.* 50: 989–1000.

Edwards, K., Johnstone, C. and Thompson, C. (1991) A simple and rapid method for the preparation of plant genomic DNA for PCR analysis. *Nucleic Acids Res.* 19: 1349.

Estelle, M.A. and Somerville, C.R. (1987) Auxin-resistant mutants of *Arabidopsis thaliana* with an altered morphology. *Mol Gen Genet.* 206: 200–206.

Fowler, T.J., Bernhardt, C. and Tierney, M.L. (1999) Characterization and expression of four proline-rich cell wall protein genes in Arabidopsis encoding two distinct subsets of multiple domain proteins. *Plant Physiol.* 121: 1081-1091.

Gendreau, E., Traas, J., Desnos, T., Grandjean, O., Caboche, M. and Höfte, H. (1997) Cellular basis of hypocotyl growth in *Arabidopsis thaliana*. *Plant Physiol.* 114: 295-305.

Hall, Q. and Cannon, M.C. (2002) The cell wall hydroxyproline-rich glycoprotein RSH is essential for normal embryo development in Arabidopsis. *Plant Cell.* 14: 1161-1172.

Hijazi, M., Velasquez, S.M., Jamet, E., Estevez, J.M. and Albenne, C. (2014) An update on post-translational modifications of hydroxyproline-rich glycoproteins: toward a model highlighting their contribution to plant cell wall architecture. *Front Plant Sci.* 5: 395.

Hoekema, A., Hirsch, P.R., Hooykaas, P.J.J. and Schilperoort, R.A. (1983) A binary plant vector strategy based on separation of vir- and T-region of the Agrobacterium tumefaciens Ti-plasmid. *Nature.* 303: 179-180.

Humphrey, T.V., Bonetta, D.T. and Goring, D.R. (2007) Sentinels at the wall: cell wall receptors and sensors. *New Phytol.* 176: 7–21.

Ihsan, M.Z., Ahmad, S.J.N., Shah, Z.H., Rehman, H.M., Aslam, Z., Ahuja, I., et al. (2017) Gene mining for proline based signaling proteins in cell wall of *Arabidopsis thaliana*. *Front Plant Sci.* 8:233.

Jakoby, M.J., Falkenhan, D., Mader, M.T., Brininstool, G., Wischnitzki, E, Platz, N., et al. (2008) Transcriptional profiling of mature Arabidopsis trichomes reveals that NOECK encodes the MIXTA-like transcriptional regulator MYB106. *Plant Physiol.* 148: 1583-1603.

Kacuráková, M., Capek, P., Sasinkova, V., Weller, N. and Ebringerova, A. (2000) FT-IR study of plant cell wall model compounds: pectic polysaccharides and hemicelluloses. *Carbohydr Polym.* 43: 195-203.

Keller, B. (1993) Structural cell wall proteins. *Plant Physiol.* 101: 1127-1130.

Lamport, D.T.A. and Varnai, P. (2013) Periplasmic arabinogalactan glycoproteins act as a calcium capacitor that regulates plant growth and development. *New Phytol.* 197: 58-64.

Liu, X., Wolfe, R., Welch, L.R., Domozych, D.S., Popper, Z.A. and Showalter, A.M. (2016) Bioinformatic identification and analysis of extensins in the plant kingdom. *PLOS ONE.* 11: e0150177.

Lyndon, R.F. (1990) Plant Development – The Cellular Basis. Unwin, Hyman, London.

McCann, M.C., Hammouri, M., Wilson, R., Belton, P. and Roberts, K. (1992) Fourier Transform Infrared Microspectroscopy is a new way to look at plant cell walls. *Plant Physiol.* 100: 1940-1947.

Miedes, E., Suslov, D., Vandenbussche, F., Kenobi, K., Ivakov, A., Van Der Straeten, D., et al. (2013) Xyloglucan endotransglucosylase/hydrolase (XTH) overexpression affects growth and cell wall mechanics in etiolated Arabidopsis hypocotyls. *J Exp Bot.* 64: 2481–2497.

Mouille, G., Robin, S., Lecomte, M., Pagant, S. and Höfte, H. (2003) Classification and identification of Arabidopsis cell wall mutants using Fourier Transform InfraRed (FT-IR) microspectroscopy. *Plant J.* 35: 393-404.

Murashige, T. and Skoog, F. (1962) A revised medium for rapid growth and bio-assays with tobacco tissue cultures. *Physiol Plant.* 15: 473-497.

Nakagawa, T., Kurose, T., Hino, T., Tanaka, K., Kawamukai, M., Niwa, Y., et al. (2007) Development of series of gateway binary vectors, pGWBs, for realizing efficient construction of fusion genes for plant transformation. *J Biosci Bioeng.* 104: 34-41.

Peaucelle, A., Louvet, R., Johansen, J.N., Höfte, H., Laufs, P., Pelloux, J. and Mouille, G. (2008) Arabidopsis phyllotaxis is controlled by the methyl-esterification status of cell-wall pectins. *Curr Biol.* 18: 1943-1948.

Pelletier, S., Van Orden, J., Vissenberg, K., Delacourt, J., Urbain, A., Mouille, G., et al. (2010) Transcript profiling reveals a role for pectin de-methylesterification in the growth acceleration in dark-grown Arabidopsis hypocotyls. *Plant J.* 188: 726-739.

Pierleoni, A., Martelli, P.L. and Casadio R. (2008) PredGPI: a GPI-anchor predictor. *BMC Bioinformatics.* 9: 392.

Réfrégier, G., Pelletier, S., Jaillard, D. and Hofte, H. (2004) Interaction between wall deposition and cell elongation in dark-grown hypocotyl cells in Arabidopsis. *Plant Physiol.* 135: 959-968.

Phyo, P., Wang, T., Xiao, C., Anderson, C.T. and Hong, M. (2017) Effects of pectin molecular weight changes on the structure, dynamics, and polysaccharide interactions of primary cell walls of Arabidopsis thaliana: insights from solid-state NMR. *Biomacromolecules.* 18: 2937–2950.

Scheres, B., Wolkenfelt, H., Willemsen, V., Terlouw, M., Lawson, E., Dean, C. and Weisbeek, P. (1994) Embryonic origin of the Arabidopsis primary root and root meristem initials. *Development.* 120: 2475-2487.

Scholl, R.L., May, S.T. and Ware, D.H. (2000) Seed and molecular resources for Arabidopsis. *Plant Physiol.* 124: 1477-1480.

Séné, C.F.B., McCann, M.C., Wilson, R.H. and Grinter, R. (1994) Fourier-Transform Raman and Fourier-Transform Infrared Spectroscopy: an investigation of five higher plant cell walls and their components. *Plant Physiol.* 106: 1623-1631.

Shirsat, A.H., Bell, A., Spence, J., Harris, J.N. (1996) The *Brassica napus* EXTA extensin gene is expressed in regions of the plant subject to tensile stresses. *Planta.* 199: 618–624.

Showalter, A.M., Bell, J.N., Cramer, C.L., Bailey, J.A., Varner, J.E. and Lamb, C.J. (1986) Accumulation of hydroxyproline-rich glycoprotein mRNAs in biologically stressed cell cultures and hypocotyls. In *Biology and*

Molecular Biology of Plant-Pathogen Interactions. Edited by Bailey J.A., NATO ASI Series (Series H: Cell Biology). Springer, Berlin, Heidelberg

Showalter, A.M., Keppler, B., Lichtenberg, J., Gu, D. and Welch, L.R. (2010) A bioinformatics approach to the identification, classification, and analysis of hydroxyproline-rich glycoproteins. *Plant Physiol.* 153: 485-513.

Suslov, D. and Verbelen, J.P. (2006) Cellulose orientation determines mechanical anisotropy in onion epidermis cell walls. *J Exp Bot.* 57: 2183–2192.

Suslov, D., Ivakov, A., Boron, A.K. and Vissenberg, K. (2015). *In vitro* cell wall extensibility controls age-related changes in the growth rate of etiolated *Arabidopsis* hypocotyls. *Funct Plant Biol* 42: 1068-1079.

Tamura, K., Peterson, D., Peterson, N., Stecher, G., Nei, M. and Kumar, S. (2011) MEGA5: Molecular evolutionary genetics analysis using maximum likelihood, evolutionary distance, and maximum parsimony methods. *Mol Biol Evol.* 28: 2731–2739.

Tan, L., Tees, D., Qian, J., Kareem, S. and Kieliszewski, M.J. (2018) Intermolecular interactions between glycomodules of plant cell wall arabinogalactan-proteins and extensins. *Cell Surf.* 1: 25-33.

Tierney, M.L., Wiechert, J. and Pluymers, D. (1988) Analysis of the expression of extensin and p33-related cell wall proteins in carrot and soybean. *Mol Gen Genet.* 211: 393–399.

Vembar, S.S. and Brodsky, J.L. (2008) One step at a time: endoplasmic reticulum-associated degradation. *Nat Rev Mol Cell Biol.* 9: 944-957.

Verbelen, J-P., Foubert, S., Kerstens, S., Olyslaegers, G., Quélo, A-H., Van Gestel, K. and Vissenberg, K. (2001) The onion and the student: a fruitful combination! *J Biol Educ.* 35: 196-200.

Wilson, R.H., Smith, A.C., Kacuráková, M., Saunders, P.K., Wellner, N. and Waldron, K.W. (2000) The mechanical properties and molecular dynamics of plant cell wall polysaccharides studied by Fourier-Transform Infrared Spectroscopy. *Plant Physiol.* 124: 397-406.

Winter, D., Vinegar, B., Nahal, H., Ammar, R., Wilson, G.V. and Provart, N.J. (2007) An "Electronic Fluorescent Pictograph" browser for exploring and analysing large-scale biological data sets. *PloS One* 2: e718.

Ye, Z. and Varner, J. (1991) Tissue-specific expression of cell wall proteins in developing soybean tissues. *Plant Cell*. 3: 23-37.

Xiao, C., Barnes, W.J., Zamil, M.S., Yi, H., Puri, V.M. and Anderson, C.T. (2017) Activation tagging of Arabidopsis POLYGALACTURONASE INVOLVED IN EXPANSION2 promotes hypocotyl elongation, leaf expansion, stem lignification, mechanical stiffening, and lodging. *Plant J.* 89: 1159–1173.

Xiao, C., Somerville, C. and Anderson, C.T. (2014) POLYGALACTURONASE INVOLVED IN EXPANSION1 functions in cell elongation and flower development in Arabidopsis. *Plant Cell.* 26: 1018–1035.

Zhang, Z., Li, Q., Li, Z., Staswick, P.E., Wang, M., Zhu, Y. and He, Z. (2007) Dual regulation role of GH3.5 in salicylic acid and auxin signaling during Arabidopsis-Pseudomonas syringae interaction. *Plant Physiol.* 145: 450-464.

Zhang, Y., Yang, J. and Showalter, A.M. (2011) AtAGP18, a lysine-rich arabinogalactan protein in Arabidopsis thaliana, functions in plant growth and development as a putative co-receptor for signal transduction. *Plant Signal Behav.* 6: 855-857.

TABLES

Table 1. List of ordered T-DNA lines and primers used for genotyping.

Gene locus	NASC number	SALK number	Left border gene specific primer 5' to 3'	Right border gene specific primer 5' to 3'
At1g70990	N663130	SALK_082991C	CGATTTGTAATTGCGTTTTCG	GCGTTGATGATCATTGGAAAC
	N666962	SALK_106180C	TTATTTCAGCCCATTGAGTCG	GCGTTGATGATCATTGGAAAC
	N65726	SALK_128673	CTTTGGACCTACGTTTTGGTG	ATAACAACTCTCACCATGCCG

Table 2. List of primers and TaqMan probes (Life Technologies) used for promoter region amplification and qPCR analysis.

Primers used for amplifying the promoter region	
LPat1g70990	5' -GGGGACAAGTTTGTACAAAAAAGCAGGCTCATATTTGGATTTGCATCTCTAGG- 3'
RPat1g70990	5' -GGGGACCACTTTGTACAAGAAAGCTGGGTGGGACTGATATACTAGCTAGTAC- 3'
Primers used to identify the insert of promEXT33::GFP in One Shot® TOP10 Chemically Competent cells	
M13 forward primer	5' -GTAAAACGACGGCCAG- 3'
M13 reverse primer	5' -CAGGAAACAGCTATGAC- 3'
TaqMan probes used to quantify the expression level	
At1g70990	At02227288_s1
actin 8 (At1g49240)	At02270958_gH

LEGENDS TO FIGURES

Figure 1. Geno- and phenotyping of wild type and At1g70990 (EXT33) mutants.

(A-C) Mature etiolated hypocotyl length of wild type and of three independent EXT33 T-DNA insertion lines. Schematic representation of the At1g70990 (EXT33) gene structure, including start and stop-codon, one exon and (D) the T-DNA insertion positions in *ext33-1*, *ext33-2* and *ext33-3* mutants. (E) Alignment of the amino acid sequence of EXT33 and the two most related short extensins. Prolines are marked in grey shade. (F-H) Phylogenetic tree made from neighbor-joining analysis using Mega 5.05 software of the most related proteins in *Arabidopsis thaliana* (F), all *Arabidopsis* taxa (G) and all short extensins family (H) identified by BlastP. The bootstrap values are shown in the tree and 1000 replicates were used.

Figure 2. Hypocotyl and root growth phenotyping in wild type and mutants with altered *EXT33* expression levels.

(A) Expression levels of *EXT33* measured by qPCR in the abovementioned lines and expressed as fold change relative to the wild type. (B-D) Growth curves of etiolated hypocotyls of wild type and three EXT33 T-DNA insertion lines: (B) *ext33-1*, (C) *ext33-2*, (D) *ext33-3*. Hypocotyl length is expressed as mean ± SE. Asterisks indicate significant differences (Student's two-tailed t-test, $p<0.001$). Three biological replicates were measured. (E-G) Daily growth rates of three EXT33 T-DNA insertion lines and WT. (H- J) Root growth in wild type and three T-DNA insertion lines of EXT33: (H) *ext33-1*, (I) *ext33-2*, (J) *ext33-3*. Root length is expressed as mean ± SE. No significant differences were observed (Student's two-tailed t-test, $p<0.001$). Three biological replicates were measured. (K-M) Hypocotyl phenotyping of three etiolated 35S-EXT33 overexpression lines. Asterisks indicate significant differences (Student's two-tailed t-test, $p<0.001$). Three biological replicates were measured.

Figure 3. Expression pattern of *EXT33*.

Confocal analysis of transgenic seedlings bearing a promoter::GFP construct at different ages. (A) Light grown 2-day-old and (B) 5-day-old seedlings, (C) dark grown 2-day-old seedling, (D) root and (E) hypocotyl cross-section. Scale bars: 500 µm (A-C), 50µm (D), 40 µm (E).

Figure 4. Subcellular location of EXT33-GFP proteins.

Subcellular localisation of EXT33 using (A,C) spinning disk and (B,D) confocal microscopy of 35S-driven EXT33-GFP in (A) root and (B) hypocotyl cells, and in (C) root and (D) hypocotyl cells of 35S-driven EXT33-GFP reintroduced into ext33-lines. Scale bars: 20 µm. (E) Spinning disk images of co-localisation experiment of EXT33-GFP (left) and PI (middle) in etiolated hypocotyl cells. The right panel shows the merged images of the green and red channel. Scale bar: 20 µm. The lower panel shows magnifications to show the co-localisation of the GFP and PI signal. Scale bar: 3 µm

Figure 5. Composition and *in vitro* extension of wild type and EXT33 mutant cell walls.

(A-C) Student's t-tests on the difference of FT-IR spectra from (A) basal, (B) middle and (C) top parts of 4-day-old etiolated hypocotyls of T-DNA lines versus the wild type. Horizontal red lines indicate limits of the 95% confidence interval.

(D) Creep rates of 5-mm hypocotyl segments of 96h-old wild-type and two T-DNA mutants of EXT33 determined by constant load extensometry using a 600 mg load. Asterisks indicate a statistical significance versus the wild type at $P<0.015$ (t-test).

Figure 1

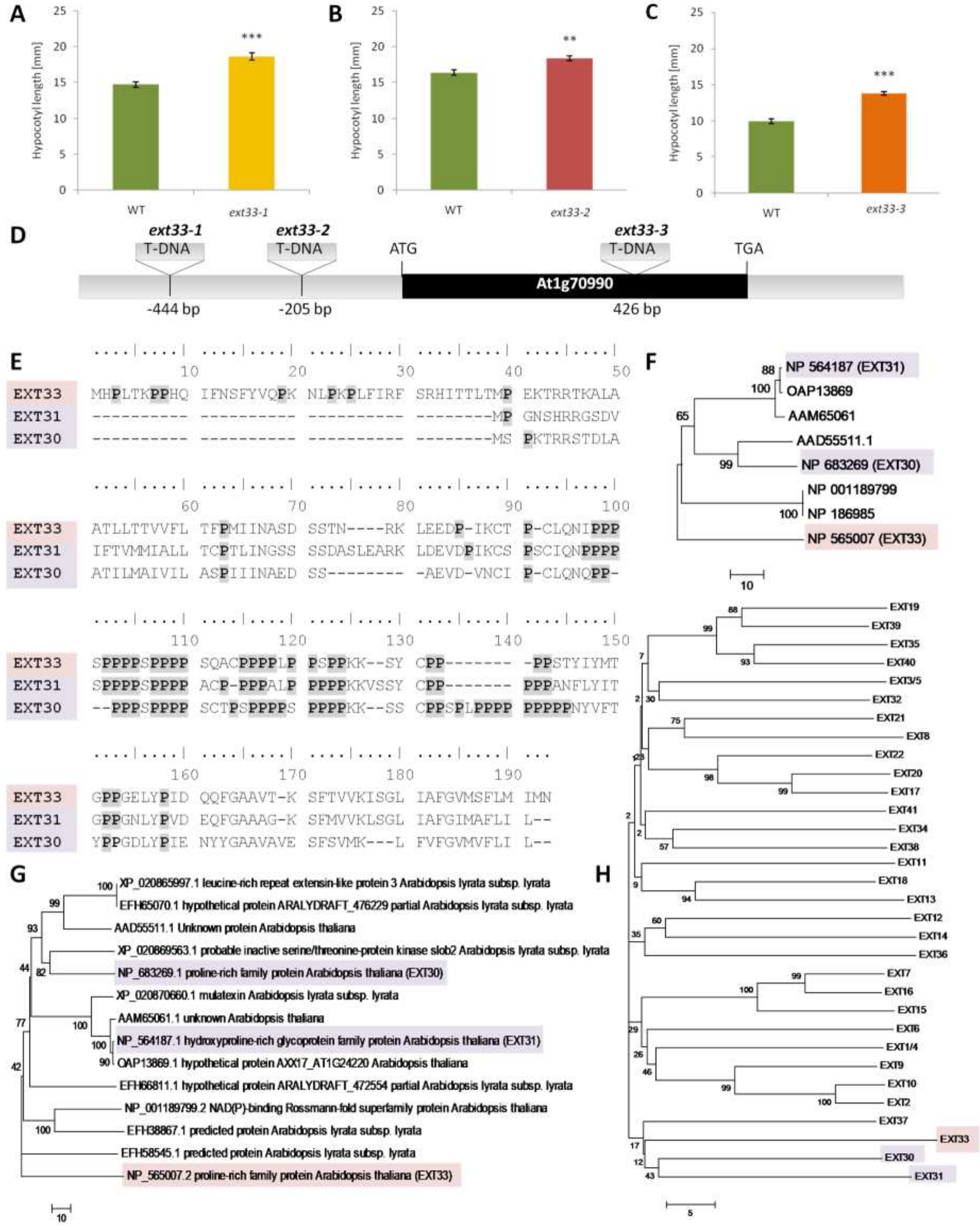

A
B
C
Hypocotyl length [mm]
WT
ext33-1
ext33-2
ext33-3
***
**
D
T-DNA
ATG
TGA
At1g70990
-444 bp
-205 bp
426 bp
E
EXT33
EXT31
EXT30
F
NP 564187 (EXT31)
OAP13869
AAM65061
AAD55511.1
NP 683269 (EXT30)
NP 001189799
NP 186985
NP 565007 (EXT33)
G
XP_020865997.1 leucine-rich repeat extensin-like protein 3 Arabidopsis lyrata subsp. lyrata
EFH65070.1 hypothetical protein ARALYDRAFT_476229 partial Arabidopsis lyrata subsp. lyrata
AAD55511.1 Unknown protein Arabidopsis thaliana
XP_020869563.1 probable inactive serine/threonine-protein kinase slob2 Arabidopsis lyrata subsp. lyrata
NP_683269.1 proline-rich family protein Arabidopsis thaliana (EXT30)
XP_020870660.1 mulatexin Arabidopsis lyrata subsp. lyrata
AAM65061.1 unknown Arabidopsis thaliana
NP_564187.1 hydroxyproline-rich glycoprotein family protein Arabidopsis thaliana (EXT31)
OAP13869.1 hypothetical protein AXX17_AT1G24220 Arabidopsis thaliana
EFH66811.1 hypothetical protein ARALYDRAFT_472554 partial Arabidopsis lyrata subsp. lyrata
NP_001189799.2 NAD(P)-binding Rossmann-fold superfamily protein Arabidopsis thaliana
EFH38867.1 predicted protein Arabidopsis lyrata subsp. lyrata
EFH58545.1 predicted protein Arabidopsis lyrata subsp. lyrata
NP_565007.2 proline-rich family protein Arabidopsis thaliana (EXT33)
H
EXT19
EXT39
EXT35
EXT40
EXT3/5
EXT32
EXT21
EXT8
EXT22
EXT20
EXT17
EXT41
EXT34
EXT38
EXT11
EXT18
EXT13
EXT12
EXT14
EXT36
EXT7
EXT16
EXT15
EXT6
EXT1/4
EXT9
EXT10
EXT2
EXT37
EXT33
EXT30
EXT31

Figure 2

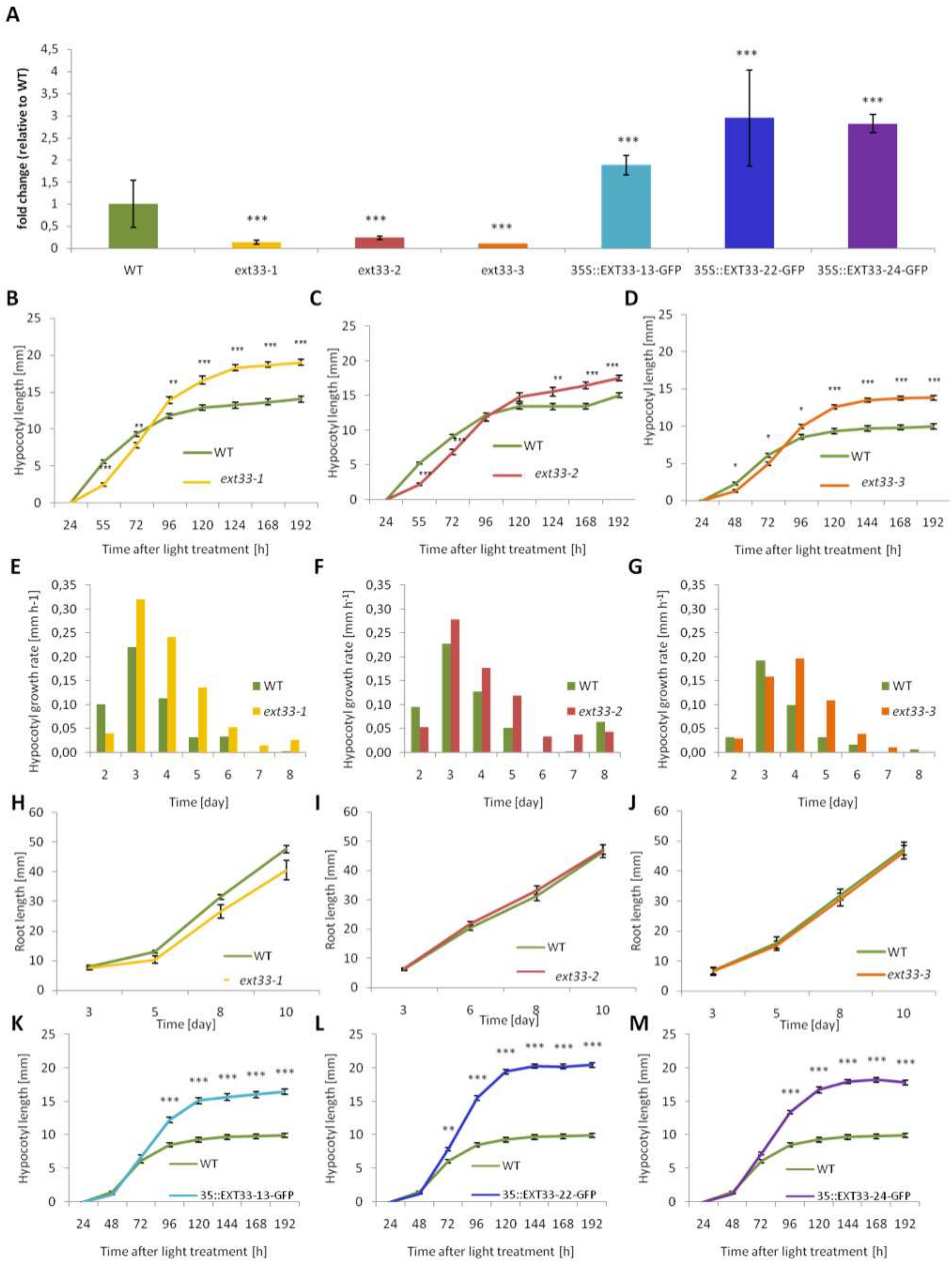
A
fold change (relative to WT)
WT
ext33-1
ext33-2
ext33-3
35S::EXT33-13-GFP
35S::EXT33-22-GFP
35S::EXT33-24-GFP
B
C
D
Hypocotyl length [mm]
Time after light treatment [h]
WT
ext33-1
ext33-2
ext33-3
E
F
G
Hypocotyl growth rate [mm h-1]
Hypocotyl growth rate [mm h-1]
Time [day]
H
I
J
Root length [mm]
Time [day]
K
L
M
35::EXT33-13-GFP
35::EXT33-22-GFP
35::EXT33-24-GFP

Figure 3

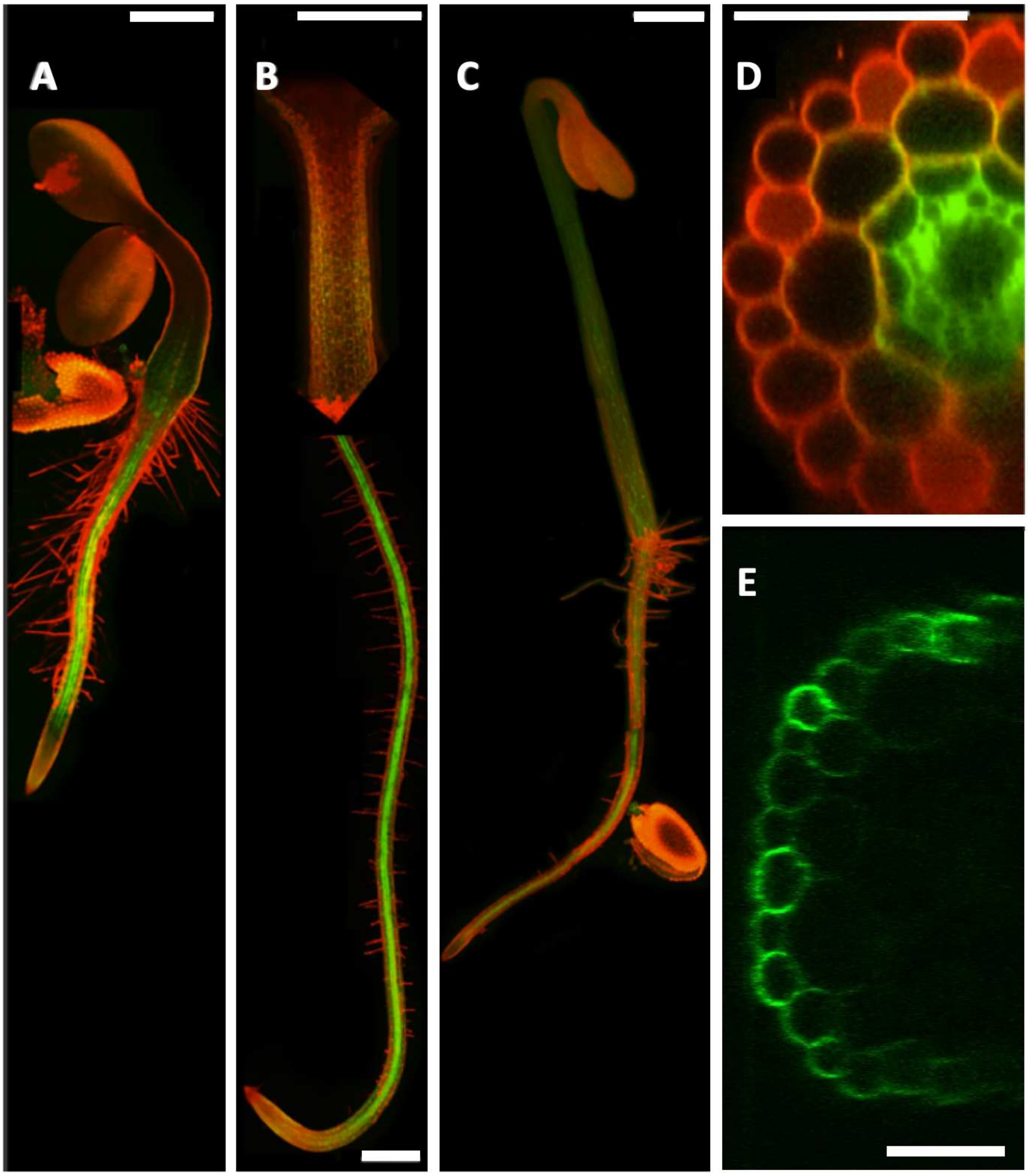

Figure 4

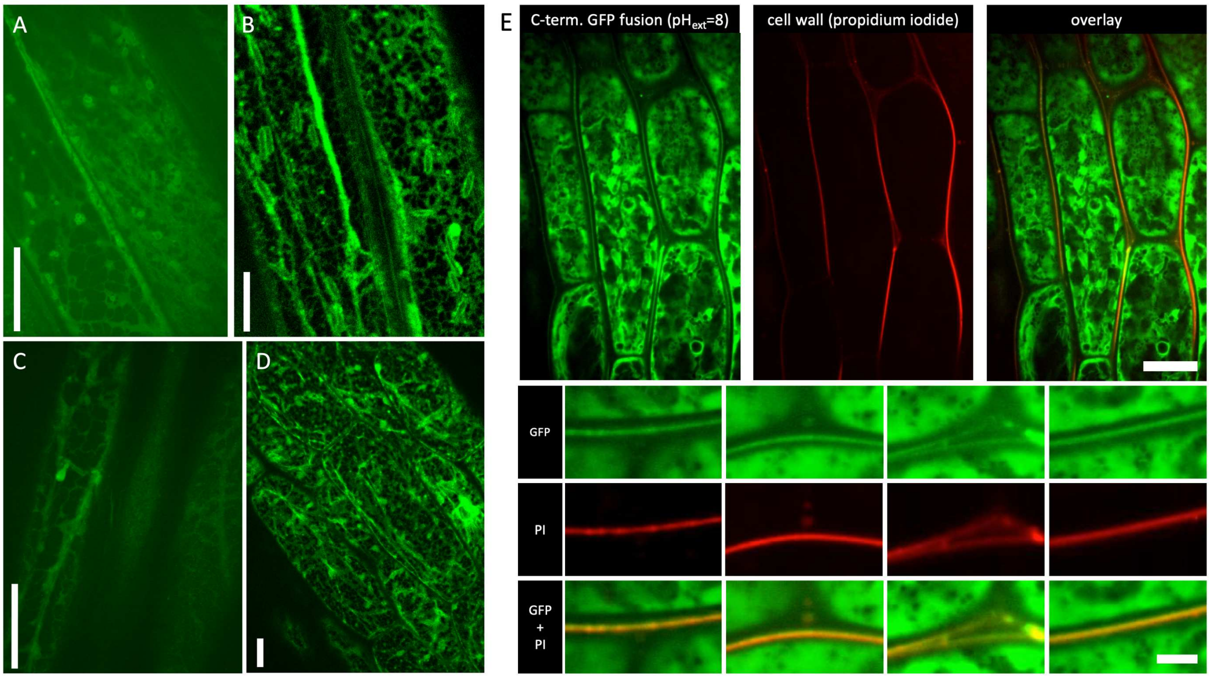
A
B
C
D
E
C-term. GFP fusion (pH_{ext}=8)
cell wall (propidium iodide)
overlay
GFP
PI
GFP
+
PI

Figure 5

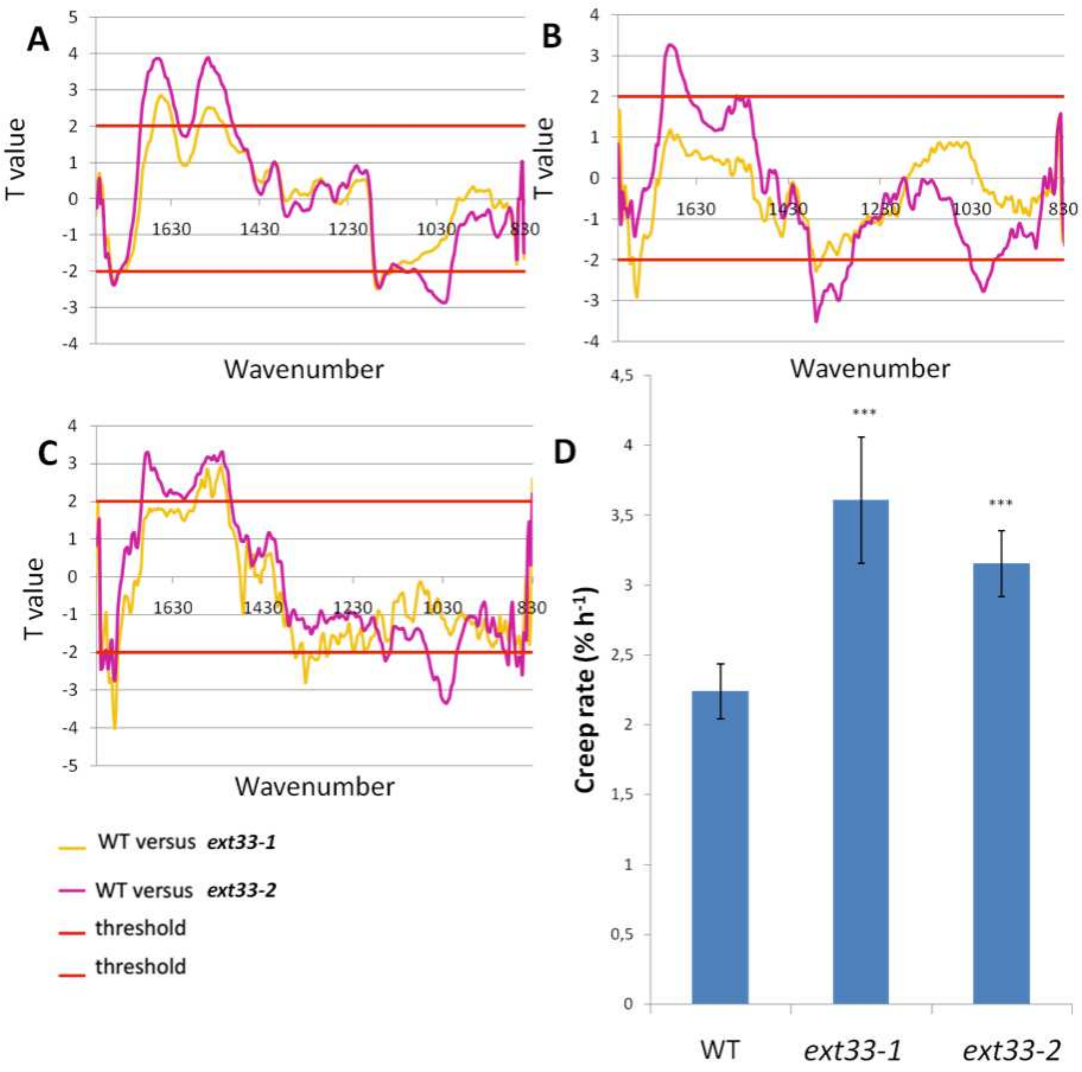
A
B
C
D
T value
Wavenumber
1630
1430
1230
1030
830
WT versus *ext33-1*
WT versus *ext33-2*
threshold
threshold
Creep rate (% h⁻¹)
WT
ext33-1
ext33-2
***

Suppl. Figure 1. Hypocotyl growth in lines with 35S::EXT33-GFP transformed in *ext33*.

(A) Growth curves of etiolated hypocotyls of two lines with EXT33-GFP introduced into *ext33* and wild type. Seedlings were grown in dark and everyday photos were taken for eight days. Hypocotyl length is expressed as mean ± SE. Asterisks indicate significant differences (Student's two-tailed t-test, $p<0.001$). Three biological replicates were measured.

(B) EXT33 expression level in reintroduced line 1 and 2 measured by qPCR and expressed relative to the expression level in the wild type.

A

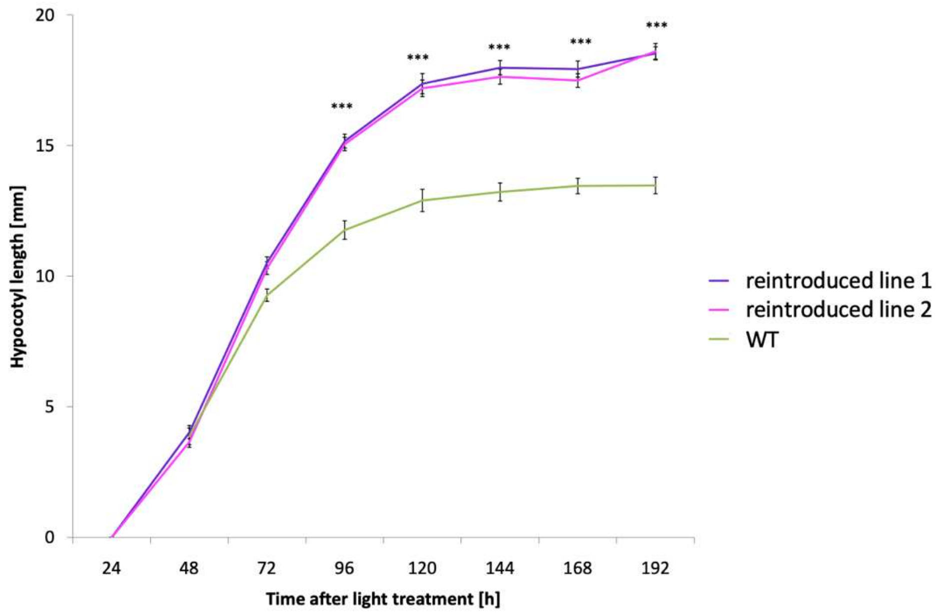

B

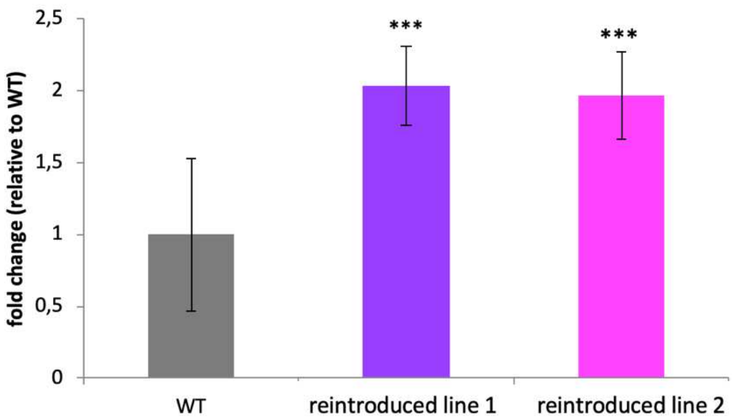

Suppl. Figure 2. Expression pattern of *EXT33* revealed by the eFP browser

eFP-browser (Winter *et al.*, 2007) retrieved expression levels of At1g70990 in different *Arabidopsis thaliana* organs, presented using color codes (A), and in the root (B).

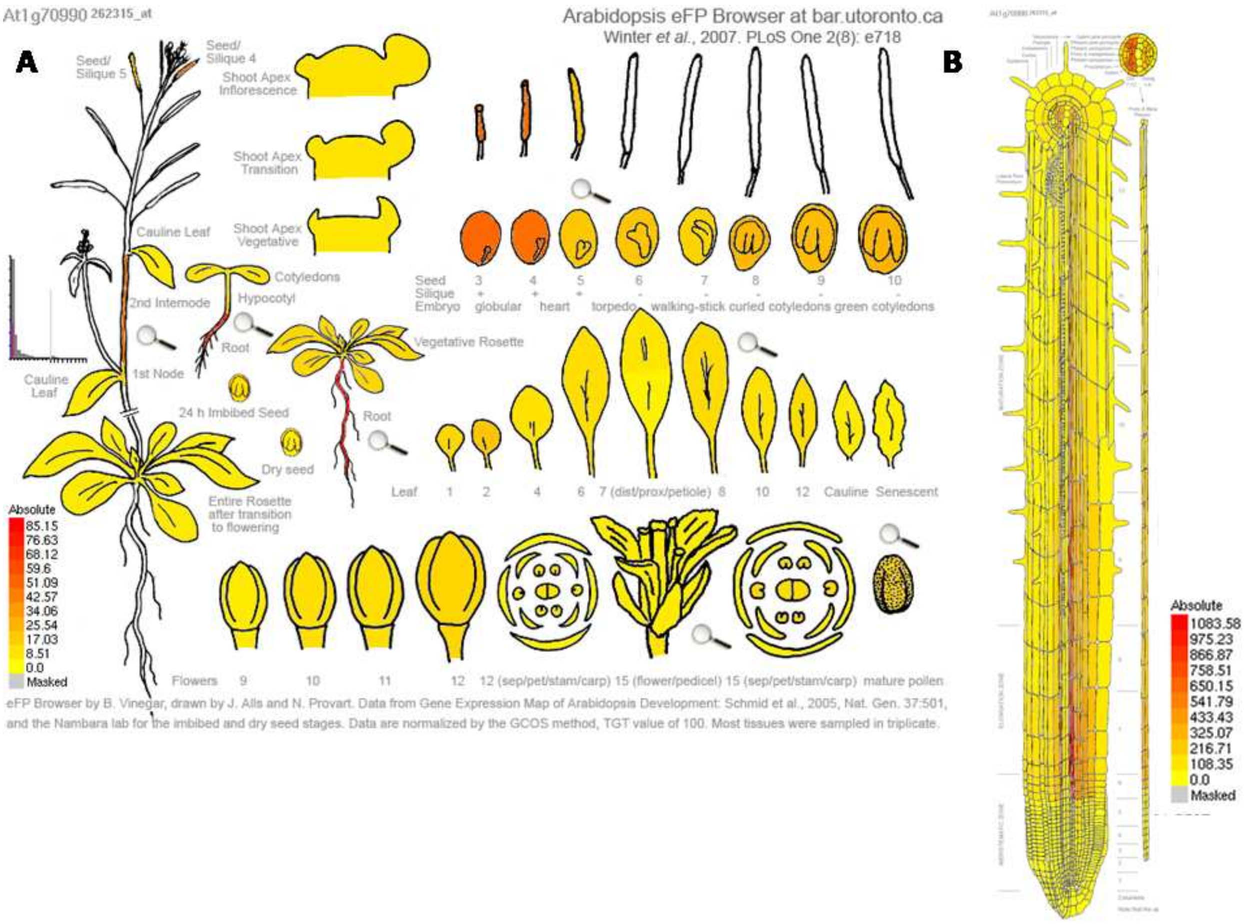

Suppl. Figure 3. Expression pattern of *EXT33* along dark-grown hypocotyls

Three representative hypocotyls of different length/ages were imaged on a Nikon AZ100 macroscope using the 0.5x objective and a 100s exposure. The average GFP signal intensity and background signal intensity were extracted along the length of the entire hypocotyl starting from the cotyledon junction. Due to the long exposure time and some light scattering a faint green background halo is visible in the middle of the image. The background subtraction fully corrects for that. The graph shows normalized (arbitrary units) background corrected GFP signal intensity for all three hypocotyls. The graph clear shows that the expression is localized to base/middle of the hypocotyl, which corresponds to the fast-growing zone at that length/age. Scale bar = 500 μm.

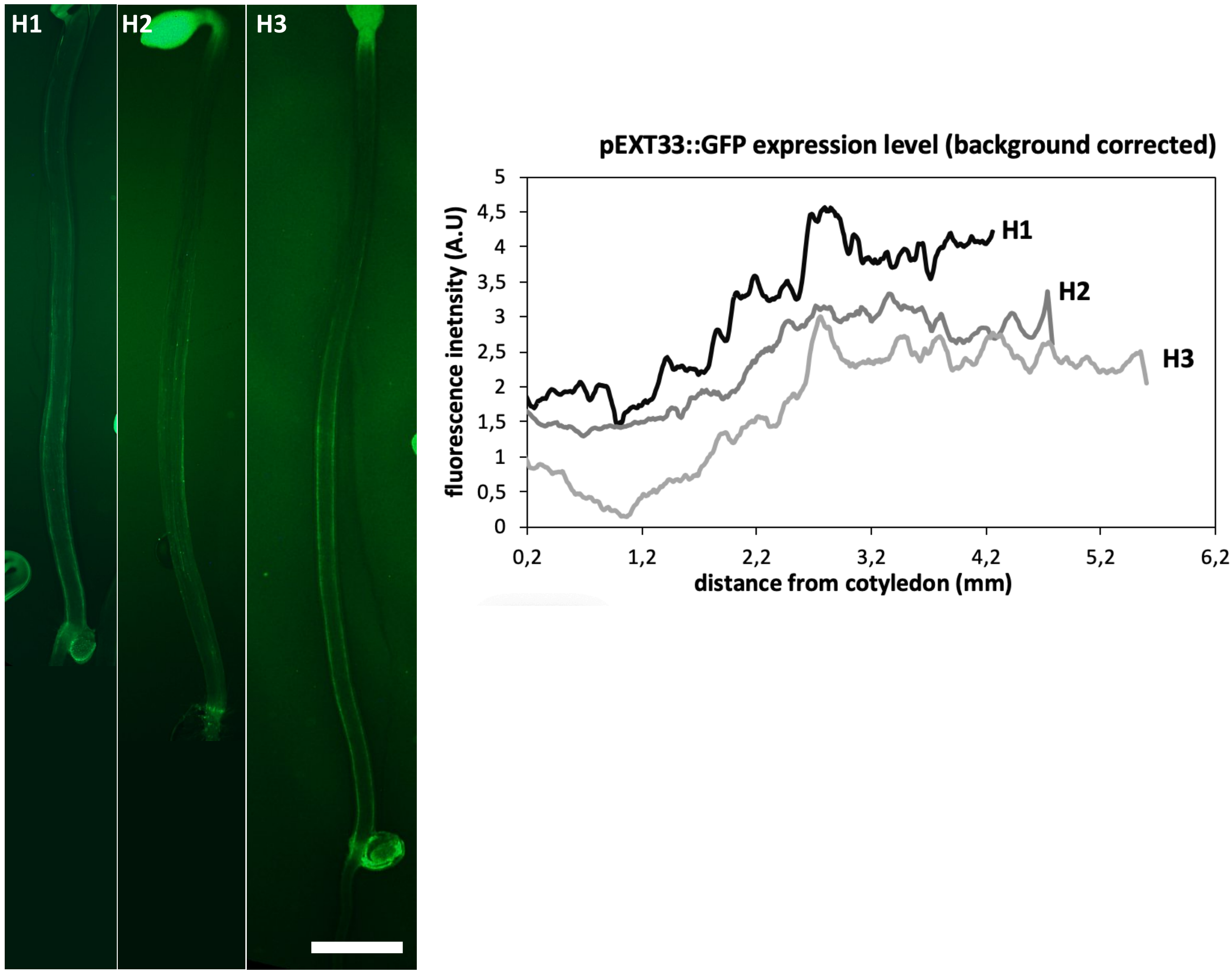

Suppl. Figure 4. ER localisation of EXT33-GFP and DioC$_6$(3)

Spinning disk images of EXT33-GFP (left) and DioC$_6$(3) staining marking the ER (right) in dark-grown Arabidopsis hypocotyl cells. Scale bar = 20μm.

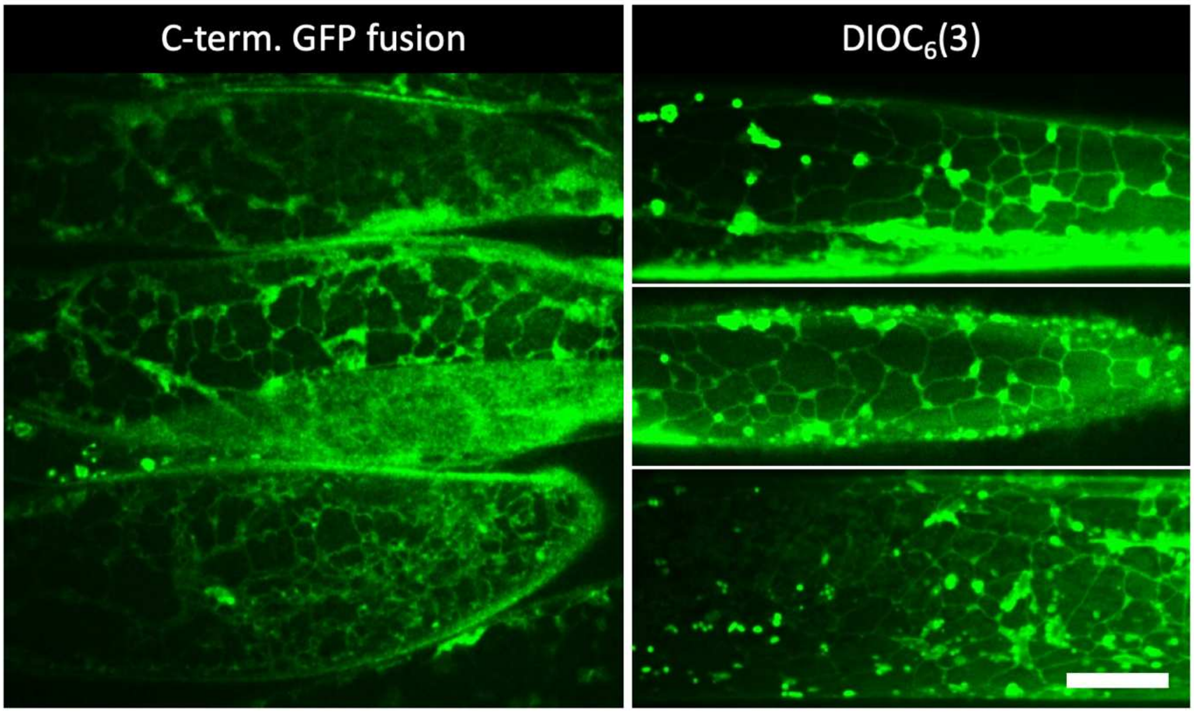

Suppl. Figure 5. Western blot analysis

Western blot analysis of proteins extracted from 2 independent lines of 35S::EXT33-GFP and probed with an anti-GFP and anti-α tubulin antibody.

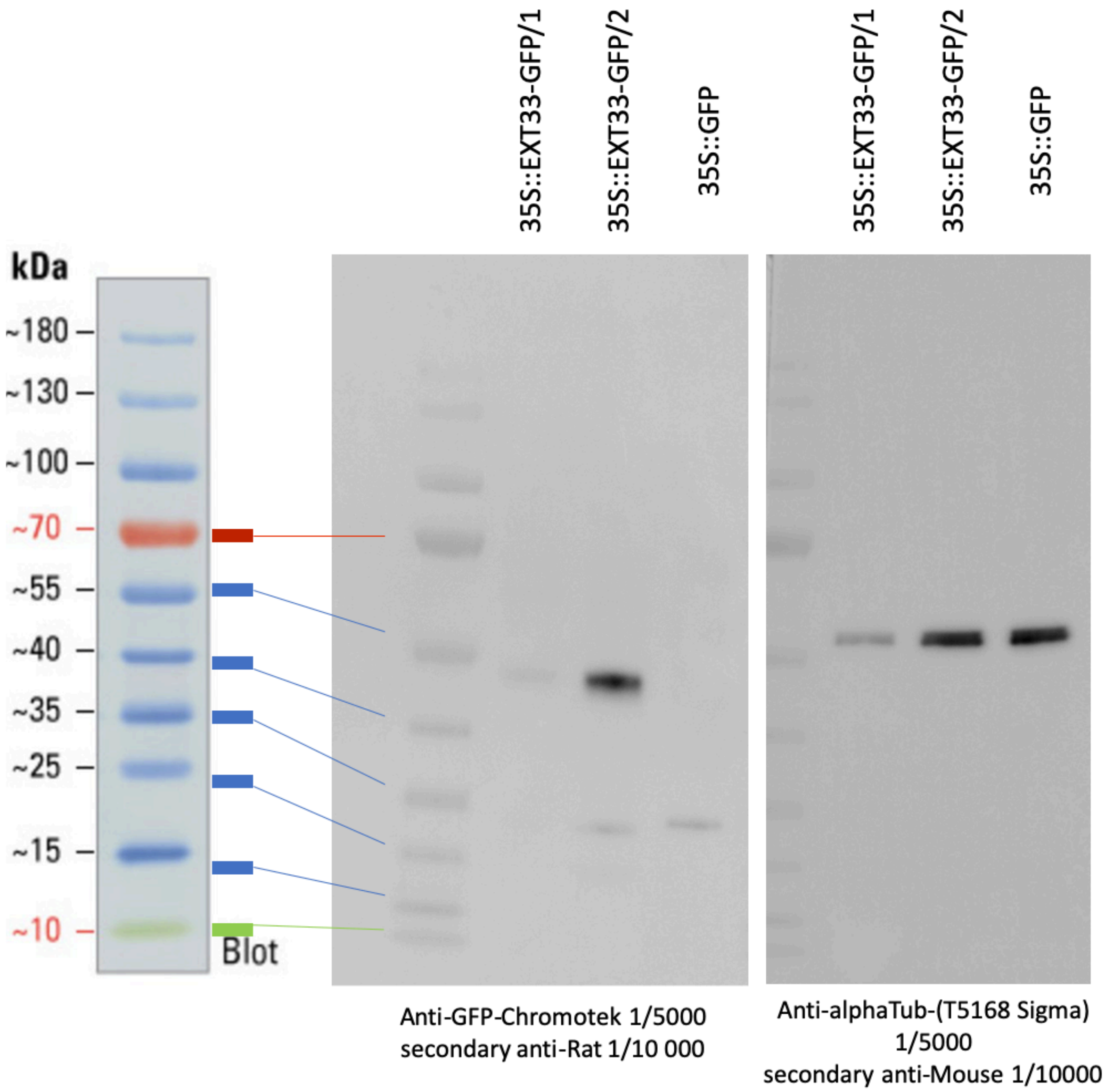

Suppl. Figure 6. Subcellular location of EXT33-GFP in relation to the nucleus.

Subcellular localisation of EXT33 using spinning disk microscopy of 35S-driven C-terminal GFP (left) and propidium iodide (middle) and a merged image (right). ER: endoplasmic reticulum, N: nucleus, CW: cell wall. Scale bar = 3 µm.